BENEMÉRITA UNIVERSIDAD AUTÓNOMA DE PUEBLA
FACULTAD DE CIENCIAS FÍSICO MATEMÁTICAS

Central production of $\pi^+\pi^-$ and $\pi^+\pi^-\pi^+\pi^-$ in diffractive processes with proton-proton collisions at 13 TeV with ALICE-LHC

Thesis presented to the College of Physics as a partial requirement for obtaining the degree of **Degree in Physics**

Presented by

Irandheny Yoval Pozos

Supervised by

Ph. D. Mario Rodríguez Cahuantzi

Puebla , Mexico

June 2020

Title: Central production of $\pi^+\pi^-$ and $\pi^+\pi^-\pi^+\pi^-$ in diffractive processes with proton-proton collisions at 13 TeV with ALICE-LHC.

Student: Irandheny Yoval Pozos

COMMITTEE

Ph. D. Arturo Fernández Telles

President

Ph. D. Eduardo Moreno Barbosa

Secretary

Ph. D. Heber Zepeda fernández

Member

Ph. D. Mario Rodríguez Cahuantzi

Advisor

Abstract

ALICE-LHC is one of the four main experiments carried out at CERN (European Organization for Nuclear Research) which is located in Switzerland near the border with France. The ALICE experiment is designed to study a phase of matter, known as quark-gluon plasma [18], but to have a better understanding of this phase, proton-proton collisions are performed which serve as a reference point for the study of heavy ion collisions. The design of ALICE has allowed studies of diffractive processes in proton-proton collisions as well as the detection of the particles produced from these processes. Therefore, data from proton-proton collisions at energies of the 13 TeV center of mass of the Run 2 of the LHC contains valuable information from diffractive processes to study the central production of $\pi^+\pi^-$ and $\pi^+\pi^-\pi^+\pi^-$ pions.

Acknowledgements

I want to thank my mom for giving me unconditional love and support all my life. To the Ph. D., Mario Rodriguez Cahuantzi for guiding and supporting me during the realization of this thesis work. To the Vice-Rectory of Research and Graduate Studies (VIEP) who supported this work through the project "Experimental study of hadronic interactions at high energies with the ALICE-LHC and MPD-NICA experiments", as well as to CONACyT for the support with the project CB CONACyT A1-S-13525 and to the Southeast National Supercomputing Laboratory.

To God

To my mother, for letting me fly

Contents

List of Tables

List of Figures

Chapter 1

Introduction

The Quantum Chromodynamics or by its acronym QCD, is the theory which allows to study the strong interactions of elementary particles and from which the properties of the hadrons are explained, so we can say, that is, through it we can understand the structure and properties of them including softQCD events as diffracive processes.

The study of diffractive processes dates back to the 16th century when Leonardo Da Vinci began to study the properties of light, but it was not until 1665 that under Grimaldi's study the phenomenon called "Diffraction" was first made known. The phenomenon of diffraction was introduced to high energy physics in the 50's by a group of scientists that included Robert Serber, Evgeniy L. Feinberg, Isaak Pomeranchunk, among others [17]. The diffractive process in particle physics is analogous to the process that occurs with light, the difference being that in high-energy physics we work with the concept of "rapidity gap" [4].

The importance of studying these interactions resides in the fact that these processes represent more than 25% of the cross section of a proton-proton inelastic collision at LHC energies [17], where we can find the four types of diffractive processes (elastic scattering, single diffraction, double diffraction and central diffraction) [4], on the other hand, the diffractive processes provide us with information about the structure of the proton as well as access to the non-disturbing processes of the QCD.

ALICE-LHC is one of the four main experiments carried out at CERN (European Organization for Nuclear Research) which is located in Switzerland near the border

with France. The ALICE experiment is designed to study a phase of matter, known as quark-gluon plasma [18], but to have a better understanding of this phase, proton-proton collisions are performed which serve as a reference point for the study of heavy ion collisions.

ALICE has an excellent program focused on the study of diffractive processes, which has allowed the study of proton-proton collisions, as well as the detection of particles produced from these processes. For this reason, data from proton-proton collisions at energies of the 13 TeV center of mass of the Run 2 of the LHC were collected in order to study the central production of 2 and 4 pions.

Chapter 2

Theoretical framework

2.1 Particle Physics

What is the world composed of? How is it organized? These, as well as many other questions have been crucial to particle physics or high energy physics, the study of the composition of matter has been very relevant to many scientists throughout history so that since the time of Democritus and the Greek atomists, man was already questioning and trying to investigate the structure of everything around him. But it was until 1897 that J.J. Thomson made known the discovery of the electron which marked a crucial point in history, since from this fact were released consecutively the discoveries of various particles such as the proton or neutron which at first were considered fundamental but over the years it has been found that the latter are composed of even smaller objects. The last century theoretical and experimental efforts have converged in the construction of the standard model theory.

2.1.1 Standard Model

The standard model theory of particles describes that the structure of matter is made up of particles called fermions, these particles interact with the fields in the same way that they act as sources of them, that is, they interact with the mediating particles, which are known as bosons. It is important to point out that fermions have the

characteristic of having a semientral spin and of dividing themselves into quarks and leptons. On the other hand, bosons have an integer spin and contain all those particles that mediate interactions: gluon,± W, Z bosons, photon and the hypothetical particle known as graviton. From the above we can see that matter is made up of three different types of particles: quarks, leptons and mediators or carrier particles.

- Leptons: In the current structure of the standard model there are six types of leptons, the electron, muon, tau and three neutrinos, to which an antiparticle is associated respectively. These antiparticles have the characteristic of having the same mass and spin, as well as having an opposite charge and magnetic moment opposite to the spin direction. Leptons are classified in three generations or families, by means of their decay, these generations have the characteristic of going from the lightest masses (first generation) to the most massive (third generation), in this way we find that the generations of leptons are ordered according to the figure 2.1

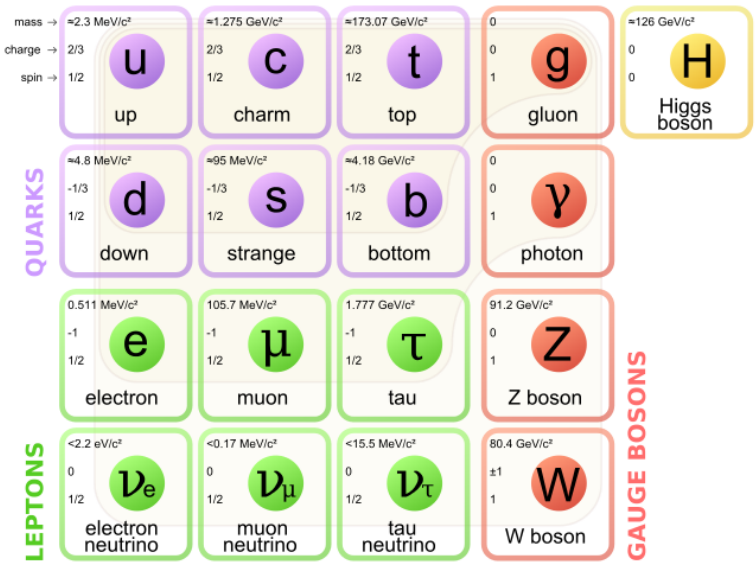

Figure 2.1: Elementary particles of the standard model

- Quarks: Like leptons, there are six types or flavors of quarks, each of which is associated with an antiparticle known as an antiquark. The quarks are classified according to their charge as: Top (T), Bottom (B), Strange (S), Charm (C), Up (U) and Down (D), these are organized equally in three generations depending on

how massive they are, currently the top quark is the most massive of all. These particles have the peculiarity of never being found in isolation, that is, they are always found in groupings called hadrons, two of the simplest systems of these hadrons correspond to:

- Baryons: Contain three quarks, for example: the proton consists of two quarks up and one quark down, as well as the neutron which has two quarks down and one quark up.
- Mesons: Contain a quark and an antiquark.

It is important to note that quarks have the characteristic of having a fractional charge, as well as having a color charge.

- Mediators: Each of the carrier particles corresponds to an interaction respectively: the photon is a carrier or mediator of the electromagnetic interaction, the $\pm W$ and Z bosons are carriers of the weak nuclear interaction, and the gluon is the mediator of the strong nuclear interaction. It is important to note that the gravitational interaction on these scales is negligible, but despite this it is thought that the hypothetical carrier particle of such an interaction is the graviton.

2.1.2 The four interactions

Within the theory of the standard model we find four interactions: strong nuclear, electromagnetic, weak nuclear and gravitational. We know that gravitational is negligible at this scale so we will focus on the other three interactions:

- Electromagnetic The electrodynamic theory is one that focuses on the study of electromagnetic forces, it was proposed by Maxwell in 1865 in the article entitled "A Dynamic Theory of the Electromagnetic Field" where he first expressed the equations that are known worldwide as "Maxwell's Equations", but the quantum electrodynamic theory (QED) emerged until the beginning of the 20th century by Feynman, Schwinger and Tomonaga.

- Weak nuclear The weak interaction exposes the disintegration of the radioactive nature as it is the disintegration beta, this theory was proposed for the first time in 1933 by Fermi who raised the decay beta, in the following years this theory was extended until arriving at its present form, these last modifications were made around 1960 by Glashow, Weinberg and Salam.

- Strong Nuclear This interaction is described by quantum chromodynamics (QCD) which was proposed in the 1970s by Wilczek, Gross and Politzer, this theory studies the interactions that occur between color-charged particles.

2.1.3 Quantum Chromodynamics

Quantum chromodynamics (QCD) is a theory that explains the strong interactions from which the properties of hadrons, such as baryons and mesons, are explained. QCD is a gauge theory that is determined by the symmetry of the SU(3) group. Within this theory each quark is associated with three fields, this can be represented by coloured triplets

$$\mathbf{q} = \begin{bmatrix} q_{red} \\ q_{green} \\ q_{blue} \end{bmatrix} \tag{2.1}$$

Where each q_i is a four component Dirac spinner and each i= red, green and blue, which indicates the states of color. It should be noted that leptons do not participate in these interactions, since the particles that have color charge are quarks and gluons. The main process in chromodynamics is given by

$$quark \rightarrow quark + gluon \tag{2.2}$$

Which is represented by the following Feynman diagram:

Another process that is important to emphasize is that in which two primitive vertices are present, such as that of the figure 2.3

It can be seen that Figure 2.3 refers to the force between two quarks mediated by the

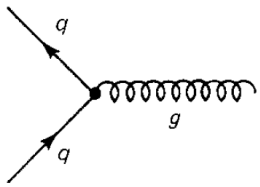

Figure 2.2: Feynman diagram for a process $quark \rightarrow quark + gluon$ [8]

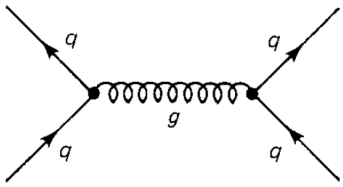

Figure 2.3: Feynman diagram with two primary vertices [8]

exchange of gluons, this type of interaction is present in the formation of baryons. On the other hand, it should be noted that gluons can be coupled with other gluons to form three gluon and four gluon vertices, as shown in Figure 2.4.

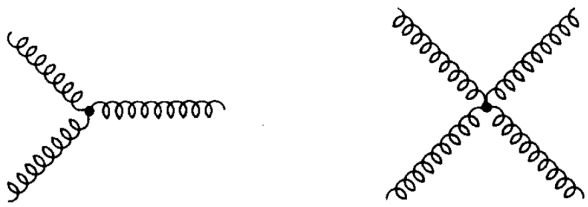

Figure 2.4: Feynman diagrams showing the coupling between three and four gluons [8]

Within QCD theory there is a coupling constant, which depends on the distance between the interacting particles and therefore on the force with which they interact. Although at the relatively large distances characteristic of nuclear physics it is big at very short distances (less than the size of a proton) it becomes quite small. This phenomenon is known as asymptotic freedom; it means that within a proton or a pion, say, the quarks rattle around without interacting much. Just such behavior was found experimentally in the deep inelastic scattering experiments. From a theoretical point of view, the discovery of asymptotic freedom rescued the Feynman calculus as a legitimate tool for QCD, in the high-energy regime [8].

This tells us that if the distance between two particles is very small the coupling

constant will also be reduced.

Returning to the idea of the first paragraph of this section, we can say that one of the objectives of this theory is to study and understand hadrons and their structure, that is why some experiments are focused on the hadron type called proton.

2.2 Diffractive Physics

The study of diffraction-related phenomena emerged in the 16th century with Leonardo Da Vinci, when he began to study the properties of light, but it was until 1665 that Grimaldi gave to know the first study of a phenomenon called "Diffraction", this term was introduced properly to the physics of particles or physics of high energies approximately in 1950 under the impulse of diverse physicists like Robert Serber, Roy J. Glauber, Isaak Ya, among others. In high energy physics this term represents an analogy with the optical effect that occurs when a beam of light hits an obstacle or crosses a slit.

2.2.1 Diffractive Processes

Today the study of diffractive processes represents a new window to new knowledge so important that experimental complexes like CERN study diffractive elastic and inelastic processes. The importance of studying these processes is due to the fact that in a proton-proton collision these phenomena represent more than 25% of the cross-section of the collision. Furthermore, from the study of these processes it is possible to deepen the understanding of the structure of the proton and the non-disturbing processes of the QCD.

Hadronics processes are classified into two types: soft processes and hard processes. The soft processes are distinguished for possessing an energy scale of the order of R ($\sim 1fm$) which refers to the order of the size of the hadrons, on the other hand, from the theoretical point of view, the Regge theory states that these phenomena are characterized by the exchange of objects called pomerons. Processes such as elastic

dispersion between hadrons and diffractive dissociation are clear examples of this type of process.

The hard processes have the characteristic of having two or more energy scales, one of them is the scale used in the soft processes, and the other is the one related to hard energy. Within these phenomena, Barone and Predazzi [4] pointed out:

"The high value of the momentum transfer allows one to use perturbative QCD. Part of the processes. however, is still of non-perturbative origin. This component is embodied in the quark and gluon distribution (or fragmentation) functions of hadrons. The so-called "factorization theorems" (Collins, Soper and Sterman 1989) ensure that the perturbative part can be separated from the non-perturbative one (p. 1). A clear example of this type of process is inelastic dispersion".

It is important to emphasize that in the last years it has been discovered that hadronics processes are immersed in diffractive processes, that is to say, that inside the diffractive processes we can find soft and hard processes at the same time.

The first definition for these processes was established in 1960 by Good and Walker, who described hadronic diffraction as

"A phenomenon is predicted in which a high energy particle beam undergoing diffraction scattering from a nucleus will acquire components corresponding to various of the virtual dissociations of the incident particles (...) These diffraction-produced systems would have a characteristic extremely narrow distribution in transverse momentum and would have the same quantum numbers of the initial particle" [4].

It is important to emphasize that from this definition we can establish the different diffractive processes:

- Elastic scattering: happens when after the collision exactly the same particles (protons) come out of the incident.

$$p + p \rightarrow p + p \tag{2.3}$$

- Single diffraction: it is similar to elastic scattering with the difference that after

the collision one of the incident protons comes out intact while the other proton breaks giving rise to other particles with the same quantum numbers.

$$p + p \rightarrow p + X \tag{2.4}$$

- Double diffraction:this process happens when both protons break after the collision giving rise to final particles with the same quantum numbers as the initial particles.

$$p + p \rightarrow X_1 + X_2 \tag{2.5}$$

- Central diffraction: in this process the protons are intact in the final state and the interaction of pomerons generates particles.

$$p + p \rightarrow p + X + p \tag{2.6}$$

Where X_1 and X_2 represent the diffractive systems.
Within the Regge theory for high energies, these phenomena are described by pomeron exchange. A pomeron is defined as "A colour singlet object with the quantum numbers of the vacuum, which dominates the elastic scattering amplitude at high energies" [6]. The Feynman diagrams corresponding to the exchange of these pomerons are shown in the following figure

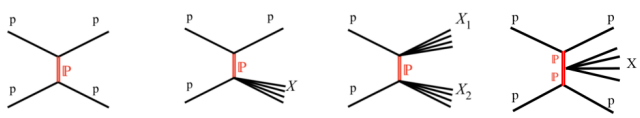

Figure 2.5: Feynman diagrams for the exchange of pomerons, the order of the diagrams is given by elastic scattering, Single Diffraction, Double Diffraction, and Central Diffraction. [21]

Given the definition of hadronic diffraction as well as its different types, it is necessary to emphasize that experimentally the results can present complications if the final particles are not reconstructed in their totality, which leads us to not know if there was an exchange of quantum numbers or not. That is why we need to know another

definition equivalent to the one exposed above but functional to practice, which is enunciated as follows:

"A diffractive reaction is characterized by a large, non exponentially suppressed, rapidity gap in the final state"[4].

Where rapidity gap refers to the space between sensitive particle detectors along the beam axis.

2.2.2 Kinematic variables

In high-energy physics, the position and momentum of particles are commonly determined by quadrivectors, which have the characteristic of remaining invariant to the Lorentz transformations.

For the study of these variables such as rapidity and pseudorapidity it is indispensable to consider that the particles collisions happen along the axis of the beam, which normally is the z-axis, with this consideration we can establish the quadrivector as

$$x = (ct, x, y, z) \tag{2.7}$$

and the quadrimoment as

$$P = \left(\frac{E}{c}, P_x, P_y, P_z\right) \tag{2.8}$$

Note that this type of notation is used because in a collider the particles do not have the same momentum but coincide in that they move in the same direction and so we can define the rapidity of a particle as [7]

$$y = \frac{1}{2}\ln\left(\frac{E + P_z c}{E - P_z c}\right) \tag{2.9}$$

Where E represents the energy and P_z the momentum of a particle along the z-axis.

From the above equation it should be noted that if the rapidity of a particle tends to zero, this would imply that the emitted particle came out in a direction almost perpendicular to the beam axis, while if the rapidity acquires a very large value it

would indicate that the emitted particle came out almost parallel to the beam axis. Note that from this rapidity information it is possible to determine the angle at which the particles are emitted after the collision.

Rapidity is considered a very useful variable because it is additionally transformed under a Lorentz impulse [4], so it can be expressed as follows

$$y \rightarrow y + \frac{1}{2} \ln \left(\frac{E + \beta}{E - \beta} \right) \tag{2.10}$$

Where $\beta = \frac{v}{c}$, while for massless particles, i.e., $E \simeq \mid p \mid$, the rapidity will be related to the angle which has the function of specifying the direction of motion of the emitted particle with respect to the z-axis, this angle is commonly called the emission angle. Knowing this, the equation of rapidity can be found as [4]

$$y = \frac{1}{2} \ln \left(\frac{1 + \cos(\vartheta)}{1 - \cos(\vartheta)} \right) = - \ln \tanh \left(\frac{\vartheta}{2} \right) \tag{2.11}$$

It is important to note that this last expression gives us the pseudorapidity (η), which is expressed as follows

$$\eta \equiv - \ln \tanh \left(\frac{\vartheta}{2} \right) \tag{2.12}$$

Pseudorapidity is an element normally used in detectors, since ϑ covers a well-defined region of the detector, this characteristic is known as acceptance.

2.2.3 Dispersion Matrix

When a collision occurs between a particle propelled through a beam and another particle moving in different directions can result, this is a clear example that shows the initial $\mid i >$ and final $\mid f >$ states of an interaction. The scattering matrix or S-matrix is defined as the linear operator which transforms the initial state $\mid i >$ of a scattering process into the final state $\mid f >$ [4].

$$S \mid i > = \mid f > \tag{2.13}$$

The states $\mid i >$ and $\mid f >$ are defined as "input" and "output", respectively. The following expression indicates the probability of the given output state as the input state

$$P_{fi} = |< f \mid S \mid i >|^2 = |< f \mid S^\dagger \mid i >||< f \mid S \mid i >| \tag{2.14}$$

Of which, if the set of orthonormal states is complete, then the relation of completeness is fulfilled.

But if we calculate the probability of going from the input state to some output state, the following expression must be validated for any set of input states and at the same time it must fulfill the completeness relation, so

$$1 = \sum f \mid< f \mid S \mid i >|^2 = \sum f \mid< f \mid S^\dagger \mid i >||< f \mid S \mid i >| =< i \mid S^\dagger S \mid i > \tag{2.15}$$

From these expressions it follows that $S^\dagger S = 1$ and $SS^\dagger = 1$. Where $S^\dagger$ represents the hermitian adjunct of S .

It is clear that by knowing the dispersion matrix in its entirety, one would have complete access to the reconstruction of the dynamics of all possible particle interactions.

It is important to note that the dispersion matrix coincides with the time evolution operator U, i.e.

$$S \equiv U(-t, t) \tag{2.16}$$

With this, Barone and Predazzi (2002) point out that *"in quantum field theory is given by the Dyson series*

$$S = 1 + \sum n = 1^\infty \frac{i^n}{n!} \int d^4x_1 ... d^4x_n \tau(H_{int}(x_1) ... H_{int}(x_n)) \tag{2.17}$$

Where H_{int} is the interaction Hamiltonian (in the representation) and

textitT denotes the time-ordered product" (p.51,52). In addition to these, this matrix has the following properties:

- Linearity
- Relativistically invariant
- Unitary
- Analyticiti
- Crossing

2.2.4 Mandelstam variables

Mandelstam variables have the characteristic of being Lorentz invariants and, at the same time, of being represented by quadrimomentum. The purpose of these variables is to provide information about particle interactions and to study the kinematics related to scattering processes.

In this section, emphasis will be put on the processes of dispersion of the type

$$1 + 2 \rightarrow 3 + 4 \tag{2.18}$$

From which we can see that this type of process arises from the reaction of two bodies and therefore from two moments given by p_1 and p_2 which interact and give as a result two other particles with moments given by p_3 and p_4, this type of process is characteristic of the s-channel.

Knowing the above, it is possible to define Mandelstam variables in the following way:

$$s = (p_1 + p_2)^2 = (p_3 + p_4)^2 \tag{2.19}$$

$$t = (p_1 - p_3)^2 = (p_2 - p_4)^2 \tag{2.20}$$

$$u = (p_1 - p_4)^2 = (p_2 - p_3)^2 \tag{2.21}$$

And for the conservation of momentum and energy, you have to

$$p_1 + p_2 = p_3 + p_4 \tag{2.22}$$

Which obey the identity [4]

$$s + t + u = \sum_{i=1}^{4} m_i^2 \tag{2.23}$$

From this expression, it is indispensable to say that only two of them are independent variables, normally taken as independent to the variables s and t, where *"s is the square of the total centar-of-mass energy and t is the squared transfered momentum"* [4]. Similarly the reactions for t and u channels are given respectively by

$$1 + \overline{3} \rightarrow \overline{2} + 4 \tag{2.24}$$

$$1 + \overline{4} \rightarrow \overline{2} + 3 \tag{2.25}$$

Where the symbol $\overline{a}$ refers to the moment of the particles involved being reversed and the quantum numbers having changed sign. The reactions of these three channels can be seen in the following figure

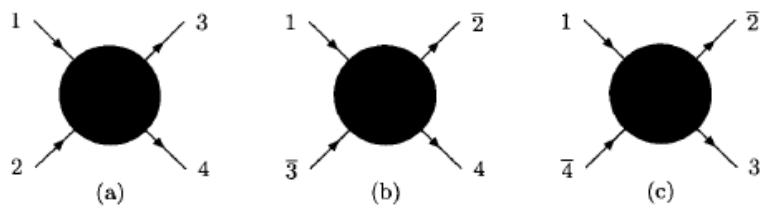

Figure 2.6: a) s-channel, b) t-channel and c) u-channel [4]

From this figure it is clear that the s,t and u processes are different from each other, "but the crossing symmetry of the S-Matrix tells us that they are described by the same scattering amplitude (or by appropriate combinations of the same amplitudes)" [4].

2.2.5 Regge Theory and Pomerons

The Regge theory was introduced to study the properties related to particles of scattering, this theory emerged in 1959 when discussing solutions to the *Schrödinger* equation for a non-relativistic scattering potential, for this, Regge proved that for one type of singularities the only singularities for the amplitude of scattering in the complex plane

were the "Regge poles".

For well behaved potentials (like the Yukawa one) the poles lie on a straight line, called the Regge trajectory. This trajectory has a form [20]

$$\alpha_R(t) = \alpha_R(0) + \alpha_{1R}(0)t \tag{2.26}$$

Where α_R is the intercept and α_{1R} the slope.

One of the trajectories presented by this theory is the so-called "Pomeron", which is responsible for increasing the cross section in collisions by increasing their energy. The experimental fit to the data from which the intercept and the slope of Pomeron were calculated was done by Donnachie and Landshoff [26]. The obtained Pomeron trajectory, with an intercept of $\alpha_R(0) = 1.08$ and a slope $\alpha_{1R}(0) = 0.25GeV^{-2}$ [20], this can be seen in figure 2.7 .

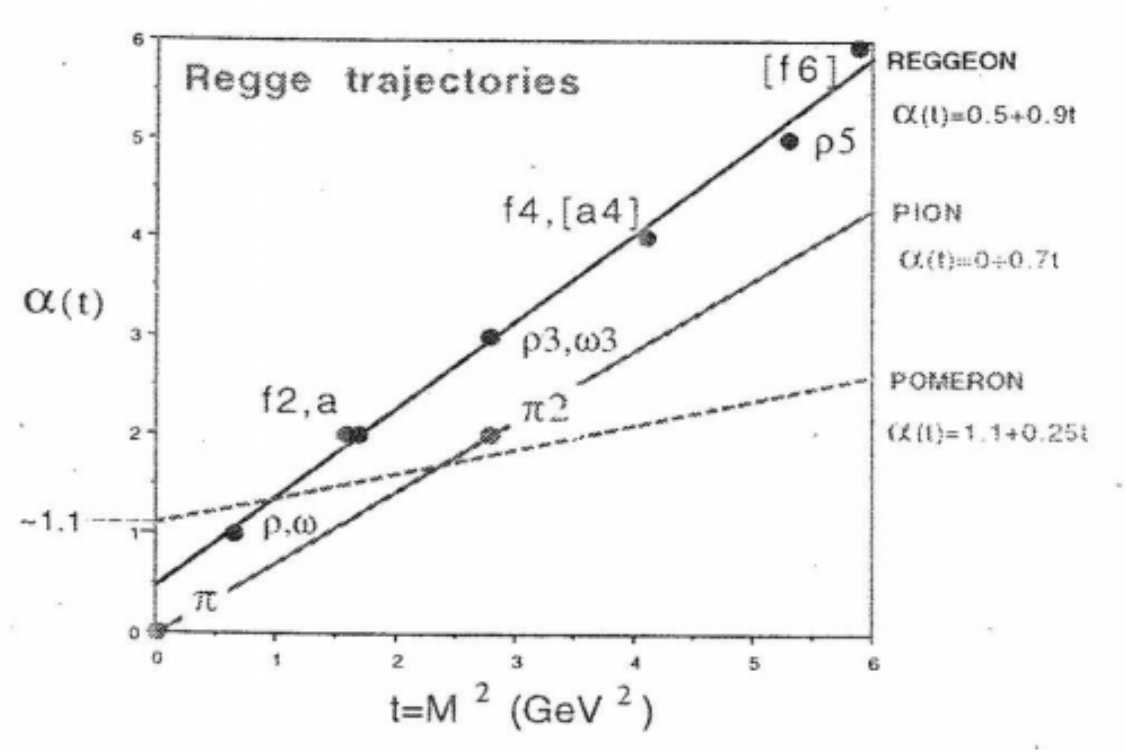

Figure 2.7: Shows the Regge trajectories [20]

2.3 Optics Previews

2.3.1 Cross Section

When two particles collide it is possible that several scenarios happen, one of them is when these objects pass so close that they only cause a change in the impulse of the same, but it can also happen that these bodies collide partially or totally producing with it several particles. The first scenario is known as elastic collision in this type of collision the kinetic energy and momentum is conserved, while the second scenario in which new particles are produced is called inelastic collision, this type of collision is characterized by conserving only the momentum or amount of movement. And it is with these two components that the cross section of the total dispersion is formed.

For the study of the cross-section, a technique known as optical wave modeling is used, which provides a fairly general description of the scattering. Now, consider a plane wave given by $\psi_i = exp(ikz)$.

We will consider the plane wave as a superposition of incoming and outgoing spherical waves, with the objective of determining the scattered wave, which is defined by the difference between the total wave and the incident

$$\psi_{scatt} = \psi_{total} - \psi_i = \frac{-iexp(ikr)}{2kr}\sum_l (2l+1)[\eta_l exp(2i\delta_l - 1]P_l(\cos\theta) = \frac{exp(ikr)}{r}F(\theta) \tag{2.27}$$

On the other hand, the solid angle obtained from the scattered outflow of a spherical surface is

$$v_0 \mid F(\theta) \mid^2 d\omega = v_0\psi^*_{scatt}\psi_{scatt}r^2 d\omega \tag{2.28}$$

Where V0 is the speed of the outgoing wave.

To find the cross section of the elastic scattering it is necessary to normalize ψ_1 and canceling V0, we obtain

$$\frac{d\sigma_l}{d\omega} =\mid F(\theta) \mid^2 \tag{2.29}$$

From which we obtain the cross-section of the total elastic dispersion

$$\sigma_l = 4\pi\lambda^2 \sum_l (2l+1) \mid \frac{exp(2i\delta_l) - 1}{2i} \mid^2 = 4\pi\lambda^2 \sum_l (2l+1) \sin^2 \delta_l \tag{2.30}$$

And the cross section of the total inelastic dispersion is

$$\sigma_{inel} = \int d\omega r^2 (\mid \psi_{in} \mid^2 - \mid \psi_{out} \mid^2) = \pi\lambda^2 \sum_l (2l+1)(1-\eta_l^2) \tag{2.31}$$

And since the total cross-section is the sum of the elastic and inelastic cross-section, we obtain

$$\sigma_{tot} = \sigma_{el} + \sigma_{inel} = 2\pi\lambda^2 \sum_l (2l+1)(1 - \eta_l \cos 2\delta_l) \tag{2.32}$$

It should be noted that the imaginary part of $F(\theta)$ is given by

$$ImF(\theta) = \frac{1}{2k} \sum_l (2l+1)(1 - \eta_l \cos 2\delta_l) P_l(\cos\theta) \tag{2.33}$$

But if we put $\theta = 0$ and $P_l = 1$ we obtain

$$ImF(0) = \frac{k}{4\pi} \sigma_{tot} \tag{2.34}$$

2.3.2 Optical Theorem

The optical theorem relates two fundamental aspects, as is the cross-section with forward scattering. "The theorem follows from very general considerations of the conservation of energy and power flow, and has its counterpart in the quantum. mechanical scattering of particles through the conservation of probability" [10].

To establish this theorem we must consider a plane wave with a vector K_0 and fields $(\vec{E}_i, \vec{B}_i)$ which incident in the vacuum by means of a scatterer that is within the surface S1. On the other hand, the dispersing fields obey

$$\vec{E} = \vec{E}_i + \vec{E}_s \tag{2.35}$$

$$\vec{B} = \vec{B}_i + \vec{B}_s \tag{2.36}$$

Note that the scatterer has the characteristic of absorbing and dissipating the energy of the incident wave. On the other hand, the power of adsorption is given by

$$P_{abs} = -\frac{1}{2\mu_0} \oint_{S_1} Re(\vec{E} \times \vec{B^*}) \cdot n' da' \tag{2.37}$$

This expression is obtained by integrating the inner component of the Poynting vector, otherwise, if we calculate the integral to the component of the Poynting vector that goes out we obtain the scattered power

$$P_{scatt} = \frac{1}{2\mu_0} \oint_{S_1} Re(\vec{E_s} \times \vec{B_s^*}) \cdot n' da' \tag{2.38}$$

With the incident wave written explicitly as [10]

$$\vec{E_i} = \vec{E_0} \epsilon_0 e^{ik_0 x} \tag{2.39}$$

$$c\vec{B_i} = \frac{1}{k} k_0 \times \vec{E_i} \tag{2.40}$$

We have that total power is expressed as follows

$$P = \frac{2\pi}{kZ_0} Im[\vec{E_0^*} \epsilon_0^* \cdot F(k = k_0)] \tag{2.41}$$

This last expression commonly represents the basic result of this theorem. It should be noted that Jackson (1998) points out that *"The total cross section t(sometimes called the extinction cross section in optics) is defined as the ratio of the total power P to the incident power per unit area,* $\frac{|E_0|^2}{2Z_0}$ *. Similarly, the normalized scattering amplitude f is defined relative to the amplitude of the incident wave at the origin as"* [10].

$$f(k, k_0) = \frac{F(k, k_0)}{E_0} \tag{2.42}$$

and using σ_t and f , the optical theorem is expressed as

$$\sigma_t = \frac{4\pi}{k} Im[\epsilon_0^* \cdot f(k = k_0] \tag{2.43}$$

This last expression, corresponds to the standard convention of quantum mechanics. It should be noted that the optical theorem reveals different points of the dispersion and absorption of electromagnetic waves for a simple dispersion.

2.4 Resonances of ρ^0

The study of the hadronic resonances allows to study the properties of the collisions between heavy ions in the quark-guon plasma stage as well as in the later ones states of its evolution. In this section the importance of the ρ^0 resonance is discussed. The ρ^0 meson presents different combinations when decaying, such is the case that we can find pions and photons immersed in the decay of this meson. Now, we focus on the decay related to a pair of pions, which can be expressed as follows

$$\rho^0 \rightarrow \pi^+\pi^- \tag{2.44}$$

The shape of the ρ^0 peak is described by the product of a relativistic p-wave Breit-Wigner function, a phase-space factor, a mass-dependent reconstruction efficiency, and a Söding interference term [13]. It is important to note that the ρ^0 spectra related to the transverse momentum have been measured for Pb-Pb collisions as well as for p-p, with $\sqrt{s_{NN}} = 2076TeV$ in the ALICE experiment [13]. This type of decay is shown in figure 2.8

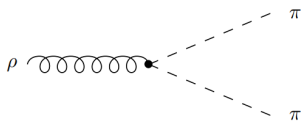

Figure 2.8: Feynman diagram describing the decay ρ^0 [14]

It can also happen that the ρ^0 meson decays into a combination of four pions, this type

of resonance is considered convenient for theories related to low energies. The first ones who studied the ρ^0 decays at four pions were Achasov and Kozhevnikon, *"they used the Weinberg Lagrangian obteined upon the nonlinear realization of chiral symmetry"* [15], with this study they adopted the ρ^0 decay, which is expressed by

$$\rho^0 \rightarrow \pi^+\pi^-\pi^+\pi^- \tag{2.45}$$

And this type of decay can be seen in the following figure

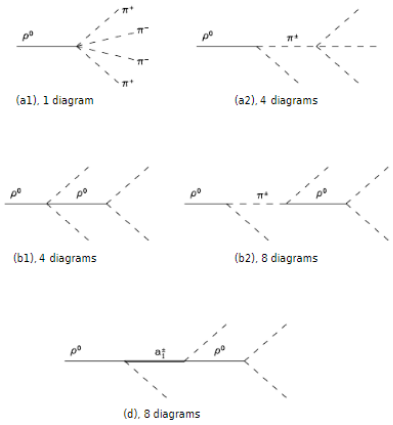

Figure 2.9: Feynman diagrams describing the decay ρ^0 [15]

The importance of studying the hadronic resonances is due to the fact that from them we can know more about the hadronic phase of the collisions with heavy ions, besides the fact that *"can also be used along with stable hadrons in studies of the mass and quark-content dependence of mechanisms that influence the shapes of particle P_T spectra"* [13].

2.4.1 Glueballs

The glueballs were proposed in the 70s, within the theory of quantum chromodynamics the quarks are confined in states of neutral color, in the same way, it admits states constituted only by gluons, which have an estimated mass of 1600 to 1800 MeV, but the certain thing is that these objects still cause much uncertainty, since diverse experiments have reported many resonances of mesons.

The truth is, the scalar glueball sector represents an opportunity to find glueball, as they have suggested that *"the scalar glueball is dissolved into the wide background into which all scalar flavour singlet mesons collapse"* [12].

2.4.2 Experimental techniques

Experimentally there are techniques to know if an resonance is a glueball, among these techniques we find

- Spin-parity determination: which is based on understanding the helicity of the two bodies arising from the reaction, i.e. when an X particle decays into other particles a and b. It is also possible that there are more than two secondary particles and in this situation it is convenient to consider the decay by grouping them in pairs. On the other hand, the amplitude of a reaction resulting in two particles is

$$\sum a_m Y_{2m}(\theta, \phi) \tag{2.46}$$

  Where a_m refers to a coefficient that depends on the states of helicity given by m, note that "it it possible to fit the distribution of decay angles θ and ϕ , and to find which Y_m choice fits the best in order to determine the spin. If the particle has spin 2, we will need to fit the unknown helicity amplitudes a_m . Usually, they will become additional unknown parameters to fit" [19].

  Another way to make these approximations is by means of the moments of the particles.

- Dalitz Plot Analysis: this technique consists in the analysis of the spin-parity of those particles that decay in three mesons, that is to say, "if a particle X decays into mesons, a, b and c, $X \to a + b + c$, it is possible that intermediate states are formed between any two of the three particles" [19], the Dalitz plot allows us to study these states, assuming that, "the invariant mass squared of two of the particles is plotted versus the invariant mass squared of a second pair of the particles" [19], in the following figure shows the Dalitz plot for two resonances

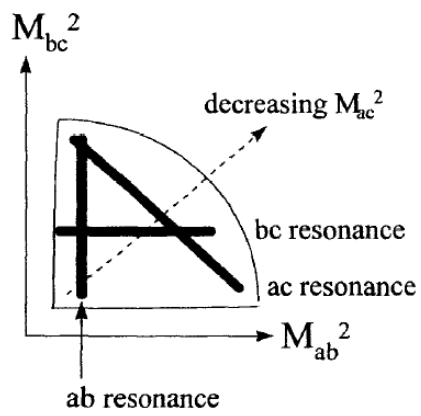

Figure 2.10: Figure of a Dalitz plot [19].

From this figure it is important to note that the density of events will depend on the spin of the intermediate particles. "The spin of a particle that decays into three mesons can be determined by trying different spin-parity hypotheses and comparing the probability for each hypothesis" [19].

2.5 ALICE Experiment

The ALICE experiment (A Large Ion Collider Experiment) is one of the four experiments along the LHC (Large Hadron Collider) which is located at CERN (Conseil Européen pour la Recherche Nucléaire). This experimental complex is located in Switzerland near the border with France.

ALICE is a heavy ion detector focused on the study of the phase of matter called quark-gluon plasma, which has a mass of 10,000 tons and measures 26 m long, 16 m high and 16 m wide, and is located in a cavern 56 m below ground.

More than 1000 scientists from over 100 physics institutes in 30 countries around the world are collaborating on this experiment.

This detector has a coordinate system given by (x,y,z), where the origin (0,0,0) of this system is located right in the center of the barrel, where the z-axis is located along the beam line, the x-axis points to the center of the LHC ring and the y-axis points upwards, orthogonally to the x-plane [21].

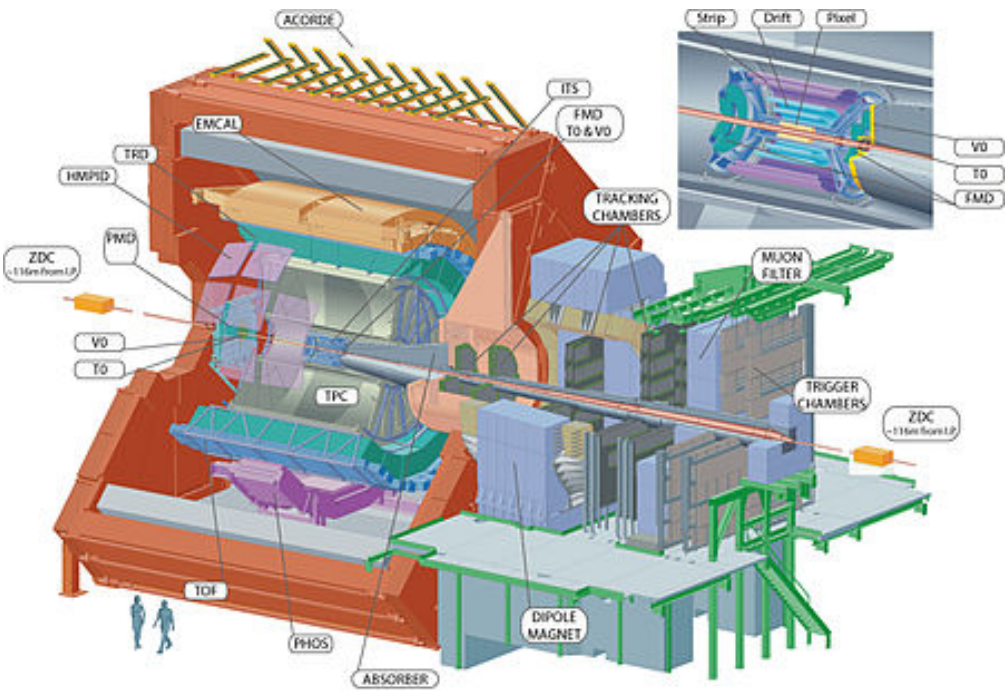

Figure 2.11: ALICE experiment

ALICE contains in the central barrel a sinusoidal shaped magnet with an intensity $B = 0.5T$, which is parallel to the z axis (along the beam direction), this magnet has the purpose of deflecting the trajectory of the particles to be able to distinguish them from each other by means of an estimation of their momentum.

This barrel has a psedurapidity region of $\mid \eta \mid < 0.9$ and at the same time contains 9 subsystems [21], the first system we will mention is the Inner Tracking System (ITS) this detector is composed of other three subsystems: SPD, SSD and SDD, this is the detector that is closer to the point of interaction, which consists of two layers for each subsystem. First we find the SPD which is able to work with very dense charged particles, besides reconstructing the secondary vertex. The SDD consist of the two middle layers of ITS, it is form by two dimensional sensors providing high resolution coordinates [21]. And finally the SSD is the most external subsystem of the ITS and its function is to match the trajectories between the ITS and the TPC. Another detector is the Time-Projection Chamber (TPC), which is "the main detector of ALICE, used for tracking and particle identification" [21]. This detector, like the ITS, has an acceptance of $\mid \eta \mid < 0.9$, and is characterized by the identification of particles through their energy deposition. It also has the TRD or Transition Radiation

Detector, which is responsible for identifying electrons in order to study light and heavy vector mesons. Another detector that is in barrel is the TOF or Time of Flight detector, which has an acceptance of $\mid \eta \mid < 0.9$ and is responsible for improving the identification of particles, making use of flight times [21]. On the other hand, there is the HMPID or High-Momentum Particle Identification Detector which allows to extend the identification of particles, while the Photon Spectrometer (PHOS) is used to detect photons. Finally we find the Electromagnetic Calorimeter (EMCAL), this detector is intended to provide trigger signals [22].

This experiment also has a muon spectrometer which has a given pseudorapidity in the range of $-2.5 < \eta < 4.0$, this spectrometer was designed to study quarkonia and light vector meson production.

2.5.1 Diffractive detectors

The ALICE experiment has a program focused on the study of diffractive processes, which has an acceptance of $-7.0 < \eta < 6.3$, this program has 6 detectors: the Forward Multiplicity Detector (FMD), the "Time 0" detector (V0), the "Vertex 0" detector (V0), the Photon Multiplicity Detector (PMD), the ALICE Diffractive Detector (AD) and the Zero Degree Calorimeter (ZDC).

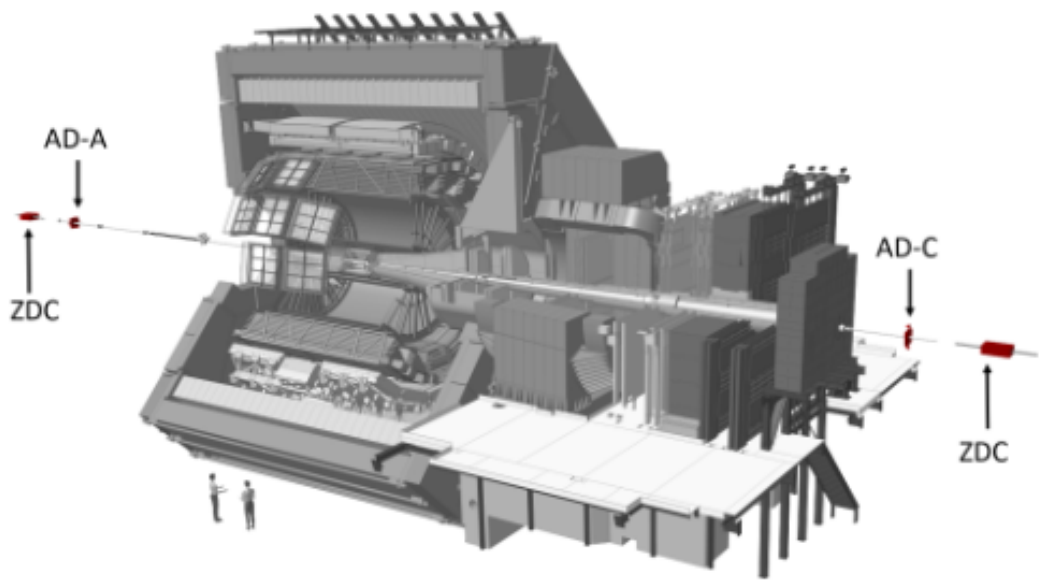

Figure 2.12: It shows the position of the AD and ZDC detectors [21]

The FMD detector is intended to study the multiplicity of charged particles in two acceptance ranges $-3.4 < \eta < -1.7$ and $1.7 < \eta < 5.1$. Another detector that composes this program is the T0 which consists of two PMTs that have Cherenkov radiators [21]. There is also the V0 detector which is made of two arrays of plastic scintillator detectors located on both sides with respect to the interaction point (V0-A at 329 cm and V0-C at 90 cm).The main goal of the V0 detector is to provide a level-0 trigger signal for ALICE to collect hadron collisions. The V0 detector is also used for centrality determination, luminosity measurements and event plane resolution. On the other hand the PMD studies the types of events and fluctuations, while the ZDC serves mainly for triggering events with proton dissociation. The last detector of this program is the AD which has the purpose of increasing the range of the pseudorapidity of this experiment and at the same time it improves the trigger of the minimum bias and diffractive events [21].

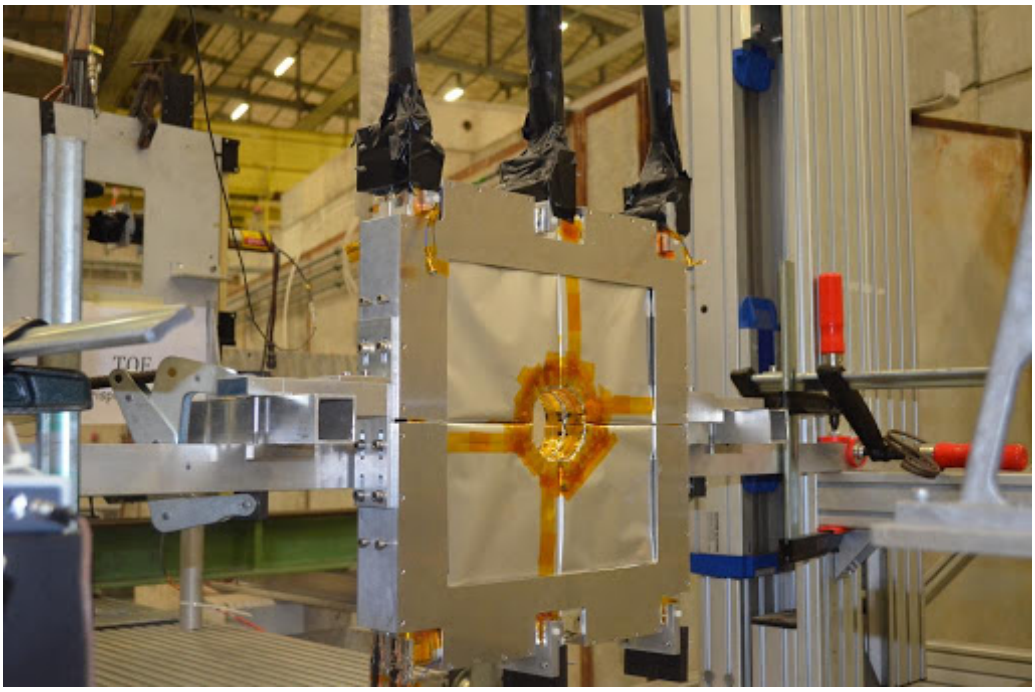

Figure 2.13: AD Detector

Chapter 3

Data Selection

3.1 Triggers employed

For the analysis of the data, the triggers CCUP13-B-SPD1-CENTNOTRD and CCUP25-B-SPD1-CENTNOTRD were used, which were active in the periods LHC17 (f, h, i, k,l, m, o, r) and LHC18 (d, e, f, g, h, j, k, l, m, n, o, p). It is important to note that the CCUP25 trigger requires the CCUP13 trigger and 2 fired TOF maxipads. Therefore, it is necessary to define that the trigger CCUP13 as follows

- !V0: veto in V0 signal detector.
- STG (SPD Topological Generalized) requires 2 tracklets with an opening angle > 54 deg
- PF (Past Future) protection in $\pm 7BCs$ (bunch crossings).

With these criterias 717 runs were selected with CCUP13 trigger and 716 runs with CCUP25 trigger for the year 2017, while for the year 2018 both CCUP13 and CCUP25 registered 661 runs which are represented in figures 3.1, 3.2, 3.3, and 3.4
On the left side show the rate given in Hz versus the run numbers per trigger per year is shown, L0b is the total number of triggers given by the detectors (hardware triggers) and L0a is the total of accepted triggers by the central trigger processor system of ALICE. On the right side, the graphs corresponding to the comparison between L2a

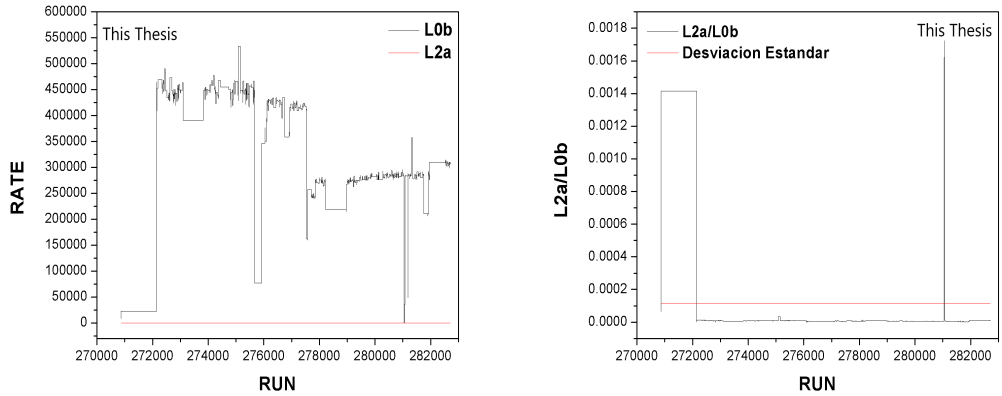

Figure 3.1: Trigger CCUP13 for the year 2017

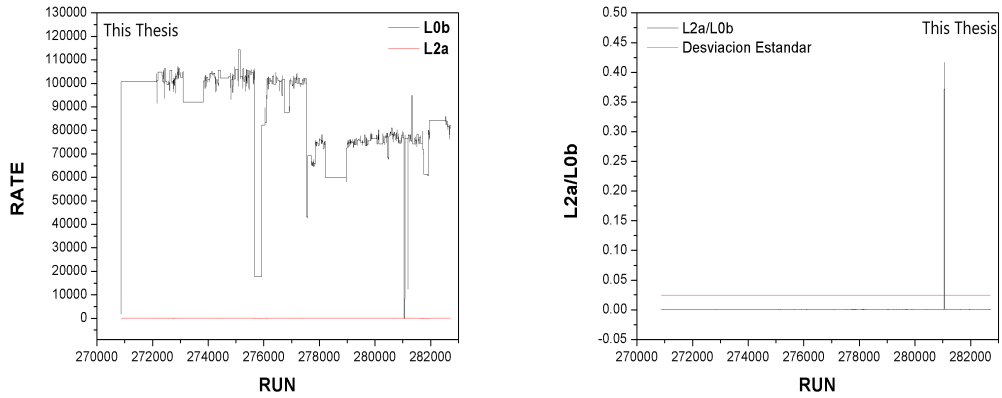

Figure 3.2: Trigger CCUP25 for the year 2017

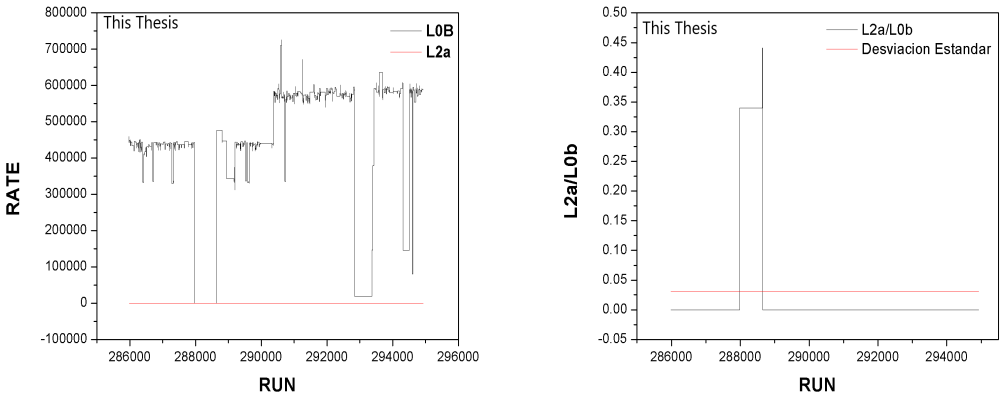

Figure 3.3: Trigger CCUP13 for the year 2018

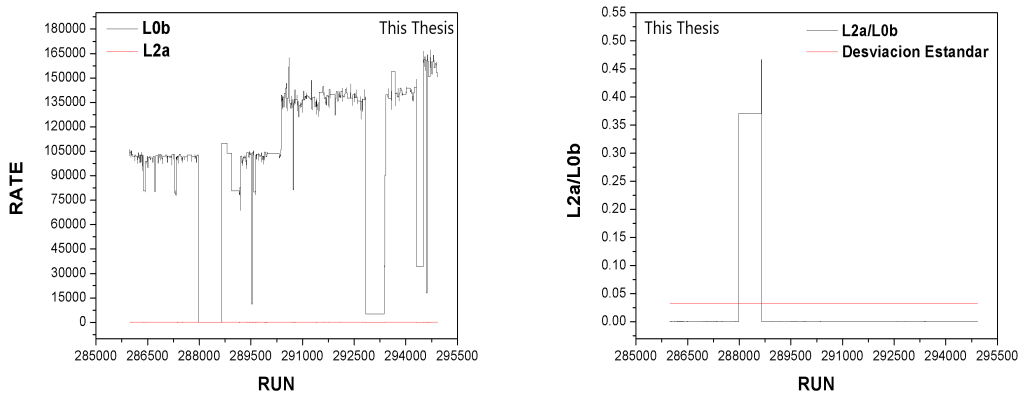

Figure 3.4: Trigger CCUP25 for the year 2018

and L0b versus collected runs are shown, where this comparison is graphed with the standard deviation of the collected data. From these last graphs we can say that a great part of the collected data when being below the standard deviation is very good with exceptions of some few that exceed this parameter.

3.1.1 Selection of runs

The selected runs of the present study belong to the years 2017 and 2018, for the selection of the same ones ALICE's LogBook was used with the following considerations:

- Time period: 01/January/2017-31/January/2017 - 01/January/2018-31/January/2018
- Beam: Yes
- Beam Type: p-p
- Beam Mode Filter: Stable Beams
- Beam Energy (GeV): Min:6499
- Data Taking Quality Flag: Good Run
- AD quality flag: not bad run
- SPD quality flag: not bad run
- TOF quality flag: not bad run

- TPC quality flag: not bad run
- V0 quality flag: not bad run

It is clear that the considerations established in the LogBook indicate that the collisions made in the years 2017 and 2018 will be studied, which are formed by protons and must be validated. The "Not bad run" indicator specified for the AD, SPD, TOF, TPC and V0 detectors ensures that the data is of good quality.
Taking into account these considerations, we proceeded to select the longest runs, which are shown in table 3.1

Run	Year	Period	Duration
286313	2018	LHC18d	10.4 h
286653	2018	LHC18e	10 h
287784	2018	LHC18f	10 h
274978	2017	LHC17k	10 h
275246	2017	LHC17k	10 h
277117	2017	LHC17l	10 h
282573	2017	LHC17r	9.9 h
286124	2018	LHC18d	9.6 h
289444	2018	LHC18l	9.5 h
277016	2017	LHC17l	9.0 h

Table 3.1: Ten longer runs

The table above shows the longest runs with their respective periods. It is necessary to remark that all the results of this work are based only in the analysis of the runs listed in table 3.1.

Chapter 4

Analysis and results

In this chapter, the results of the analysis of 2 and 4 pion events collected in diffractive processes are shown.

4.1 Reconstruction of the invariant mass

Remember that the quadrimoment of the primary particle emerging from the $\pi^+\pi^-$ and $\pi^+\pi^-\pi^+\pi^-$ pions decay channels is given by

$$p_M^\mu = p_{\pi^+}^\mu + p_{\pi^-}^\mu \tag{4.1}$$

$$p_M^\mu = p_{\pi^+}^\mu + p_{\pi^-}^\mu + p_{\pi^+}^\mu + p_{\pi^-}^\mu \tag{4.2}$$

Taking this into account, it is possible to make the reconstruction of the invariant mass from the decay channels of $\pi^+\pi^-$ and $\pi^+\pi^-\pi^+\pi^-$ pions

$$m_{2\pi}^2 = (p_{\pi^+}^\mu + p_{\pi^-}^\mu)^2 \tag{4.3}$$

$$m_{4\pi}^2 = (p_{\pi^+}^\mu + p_{\pi^-}^\mu + p_{\pi^+}^\mu + p_{\pi^-}^\mu)^2 \tag{4.4}$$

Where $m_{2\pi}^2$ and $m_{4\pi}^2$ represent the masses of $\pi^+\pi^-$ and $\pi^+\pi^-\pi^+\pi^-$ pions respectively.

4.2 Analysis for two pions

The code to analyze the experimental data sample can be found in Appendix A. For the analysis of the data, the Aliroot software with ROOT version 5.34/30 was used.

4.2.1 Cuts or kinematical considerations

To distinguish the signals of 2 and 4 pions events produced in diffractive processes from the background produced by other processes. The following list shows the cuts that were applied to the experimental data.

- PID is equal to $(\sigma_{\pi_1})^2 + (\sigma_{\pi_2})^2 < 4$
- Pt < 0.5
- !V0
- !AD
- $\mid Vtx \mid > 10$
- VtxChi2 > 100

The above restriction for the PID indicates that for this case we are asking all pairs of particles that are less than 2σ . Where the numbers $\sigma_{\pi 1}$ and $\sigma_{\pi 2}$ represent the sigma of pion 1 and pion 2, respectively. It is necessary to mention that this cut allows us to make a proper selection of pions tracks, that is why for this analysis we proceeded to make this cut in first instance, since all those data that are within the radius of 2σ are candidates to be pions, see Figure 4.2.

On the other hand, we observed that the transverse momentum Pt of two pions body is expected to be lower than 0.5 GeV/c, the same happens with the primary vertex which only considers those particles whose vertex has been reconstructed between -10 and 10 cm from the interaction point, it should be noted, that this is the range that ALICE considers for the idealized point of interaction.

In addition we required a veto in V0 and AD detectors. Finally we find the restriction in which we ask that $VtxChi2 > 100$.

Cuts	Number of events
Invariant Mass (IM)	1.185132×10^7
IM+PID	8714774
IM + PID + Pt	3244204
IM + PID + Pt +!V0	1798854
IM + PID + Pt + !V0 + !AD	839555
IM + PID + Pt + !V0 + !AD + Vtx	826393
IM + PID + Pt + !V0 + !AD + Vtx + VtxChi2	17548

Table 4.1: Cuts applied to the experimental data sample to select 2 pion events in diffractive processes.

The evolution of the invariant mass spectrum with respect to the cuts listed in table 4.1 is shown in figure 4.1, 4.2, 4.3 and 4.4

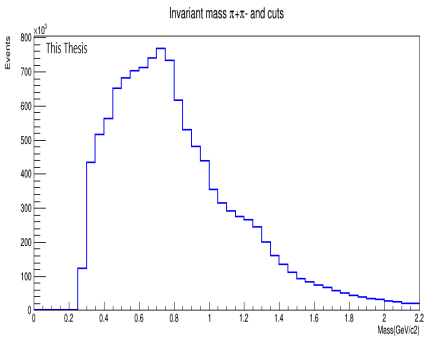

Figure 4.1: This figure shows the invariant mass (IM).

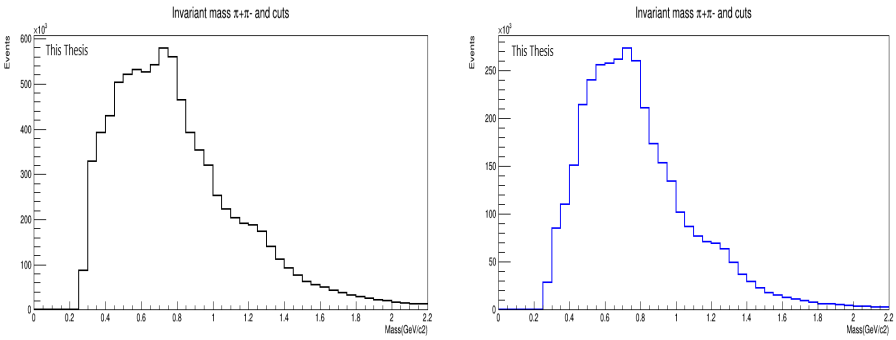

Figure 4.2: The left image shows the IM+PID cut and the right image shows the IM+PID+Pt cut.

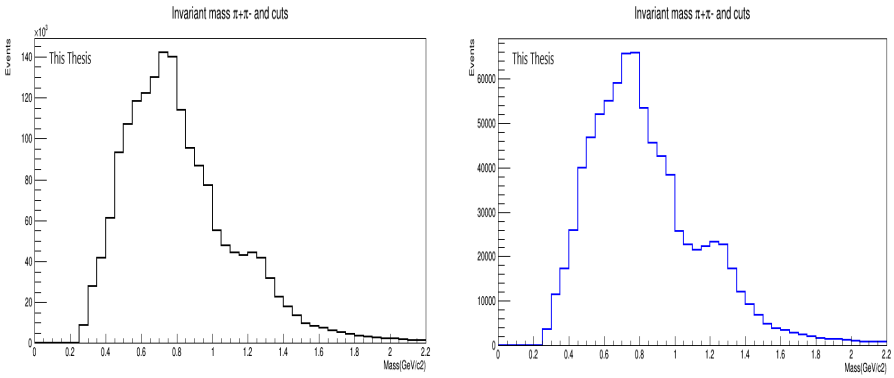

Figure 4.3: The left image shows the IM+PID+Pt+!V0 cut and the right image shows the IM+PID+Pt+!V0+!AD cut.

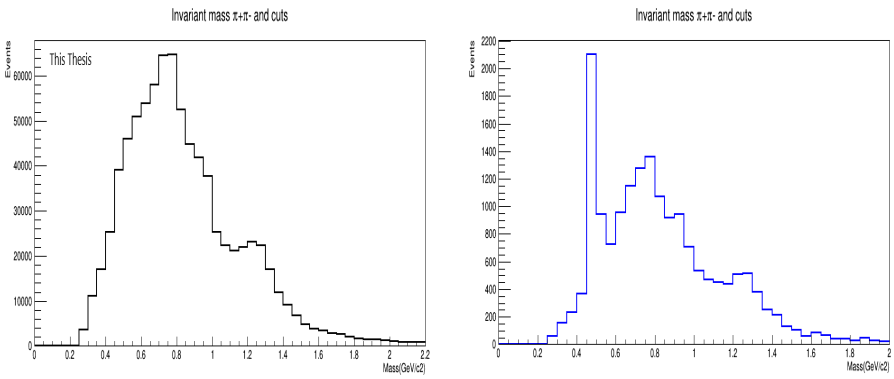

Figure 4.4: The left image shows the IM+PID+Pt+!V0+!AD+Vtx cut and the right image shows the IM+PID+Pt+!V0+!AD+Vtx+VtxChi2 cut.

The ALICE experiment has several detectors for the detection of PID or particle identification, e.g. the SDD and SSD measure the energy lost from transverse particles. But the main detector focused on the study of PID is the SSD which measures the energy loss of particles, this energy loss is well parameterized by the Bethe-Bloch formula [5]. The PID provides information about the mass and composition of particles, it should be noted that the variable normally used to discriminate is σ , which is defined as the deviation of the measured signal from the expected for a species of particle, in our case must be pions. This variable refers to a decision in which it is determined whether a certain particle belongs to a certain species of particle, from which, a certain range is assigned around an expectation of 2σ , since with this restriction the contamination of other species of particles is avoided.

In the graphs 4.5, 4.6, 4.7 and 4.8 the structures obtained for the PID using the TPC σ pion hypothesis can be seen.

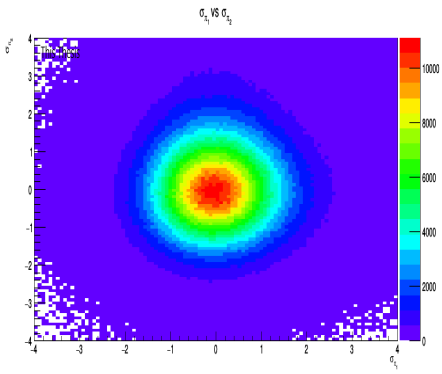

Figure 4.5: This figure shows the PID.

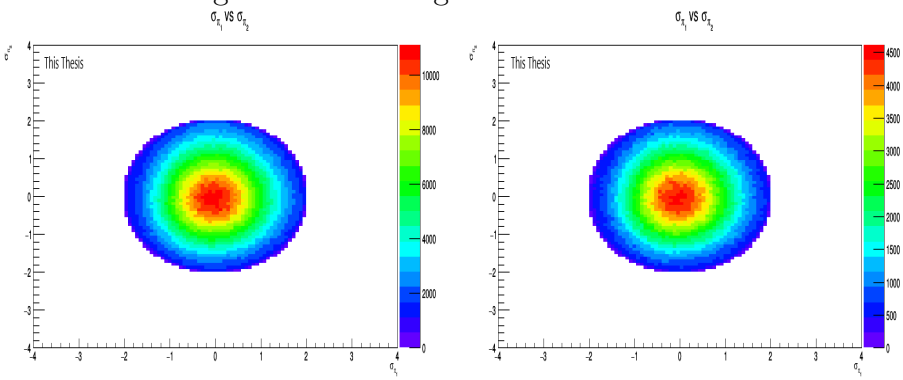

Figure 4.6: The left image shows the IM+PID cut and the right image shows the IM+PID+Pt cut.

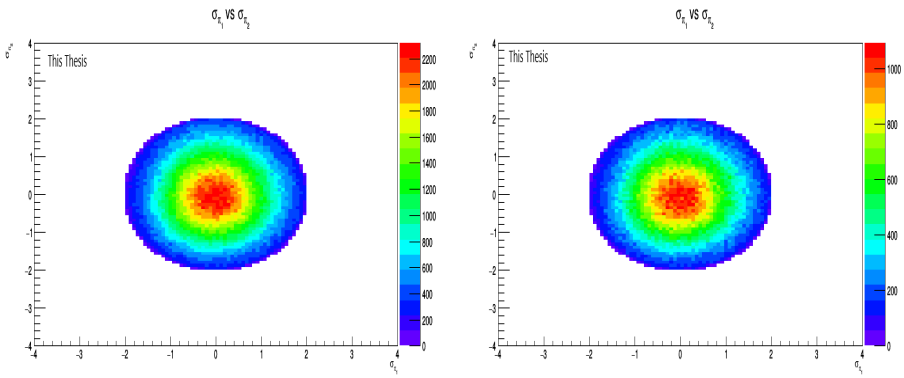

Figure 4.7: The left image shows the IM+PID+Pt+!V0 cut and the right image shows the IM+PID+Pt+!V0+!AD cut.

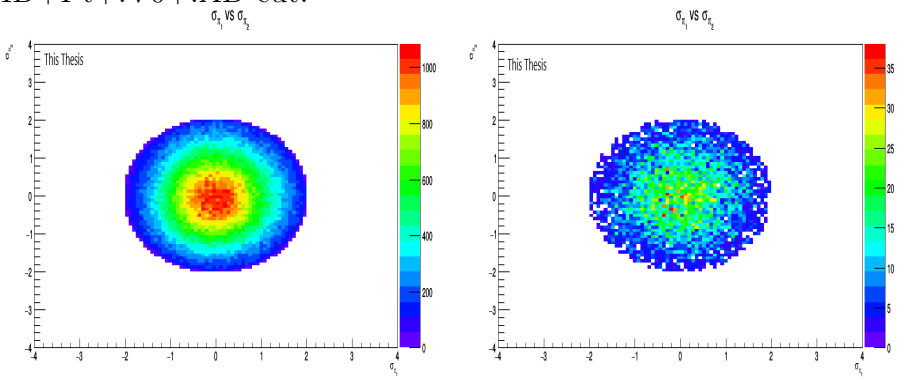

Figure 4.8: The left image shows the IM+PID+Pt+!V0+!AD+Vtx cut and the right image shows the IM+PID+Pt+!V0+!AD+Vtx+VtxChi2 cut.

Figures 4.9, 4.10, 4.11 and 4.12 show the graphs corresponding to the invariant mass vs Pt.

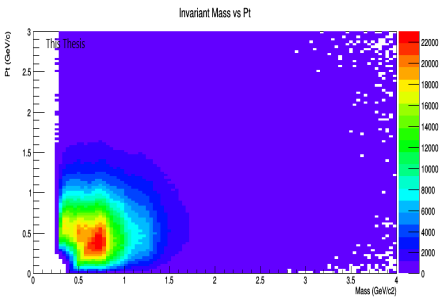

Figure 4.9: This figure shows the Invariant Mass vs Pt.

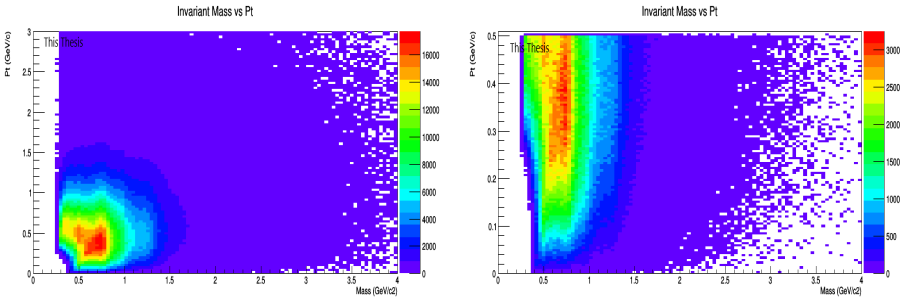

Figure 4.10: The left image shows the IM+PID cut and the right image shows the IM+PID+Pt cut.

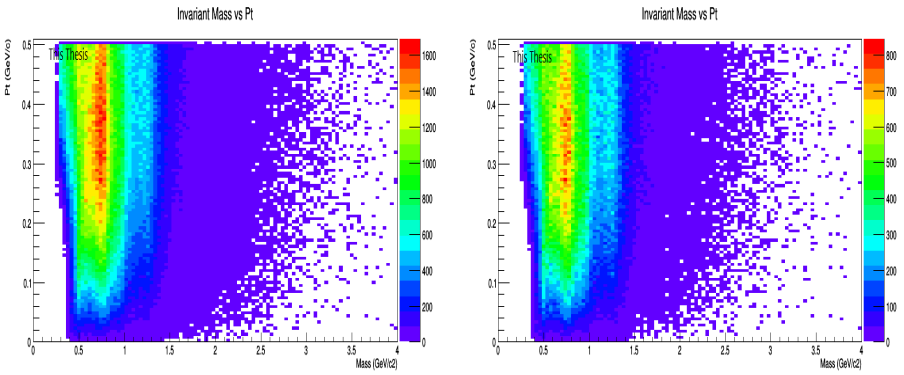

Figure 4.11: The left image shows the IM+PID+Pt+!V0 cut and the right image shows the IM+PID+Pt+!V0+!AD cut.

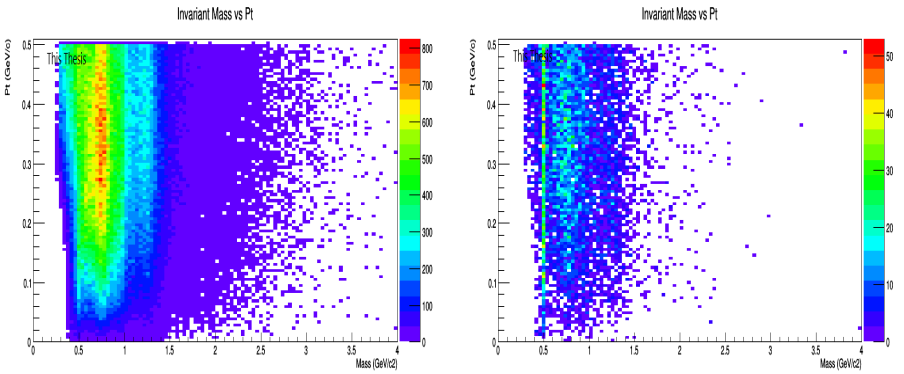

Figure 4.12: The left image shows the IM+PID+Pt+!V0+!AD+Vtx cut and the right image shows the IM+PID+Pt+!V0+!AD+Vtx+VtxChi2 cut.

Figures 4.13, 4.14, 4.15 and 4.16 show the graphs corresponding to the $Pt_{\pi_1} vs Pt_{\pi_2}$.

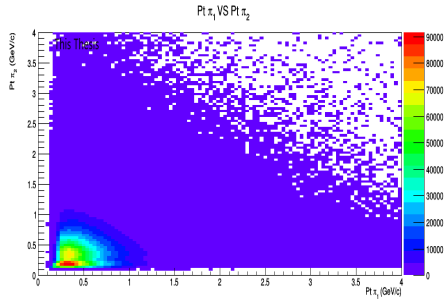

Figure 4.13: This figure shows the $Pt_{\pi_1} vs Pt_{\pi_2}$.

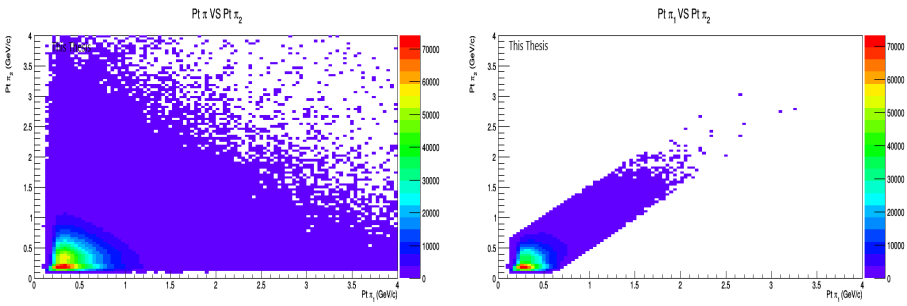

Figure 4.14: The left image shows the IM+PID cut and the right image shows the IM+PID+Pt cut.

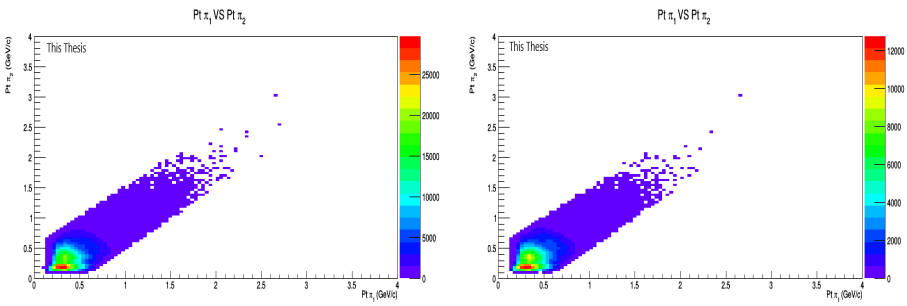

Figure 4.15: The left image shows the IM+PID+Pt+!V0 cut and the right image shows the IM+PID+Pt+!V0+!AD cut.

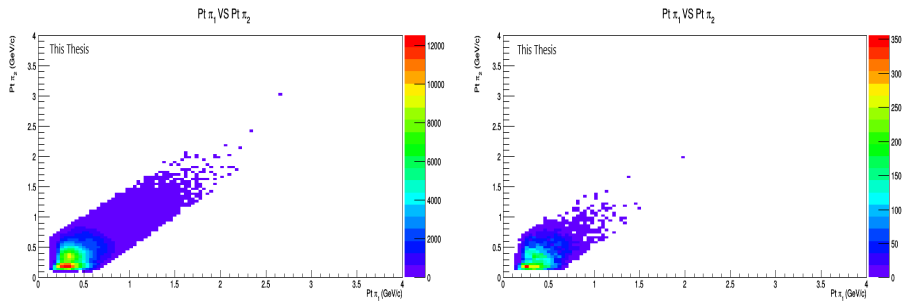

Figure 4.16: The left image shows the IM+PID+Pt+!V0+!AD+Vtx cut and the right image shows the IM+PID+Pt+!V0+!AD+Vtx+VtxChi2 cut.

Figures 4.17, 4.18, 4.19 and 4.20 show the graphs corresponding to the $\theta_{\pi_1} vs \theta_{\pi_2}$.

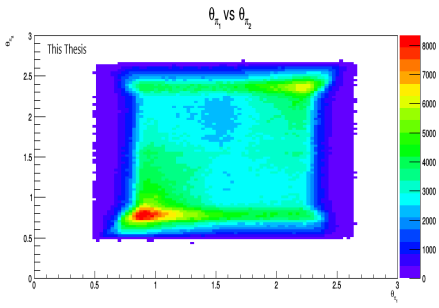

Figure 4.17: This figure shows the $\theta_{\pi_1} vs \theta_{\pi_2}$.

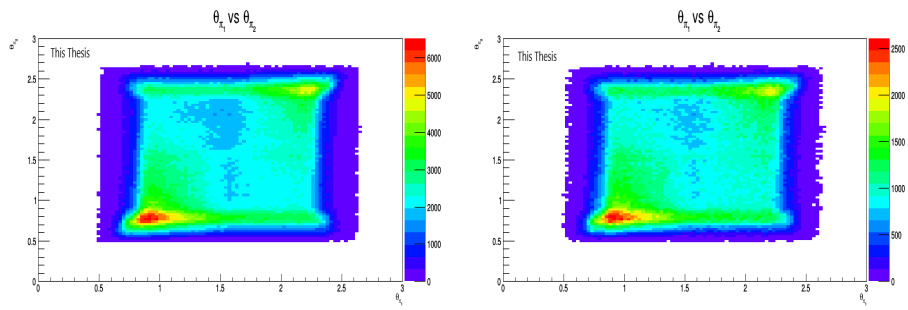

Figure 4.18: The left image shows the IM+PID cut and the right image shows the IM+PID+Pt cut.

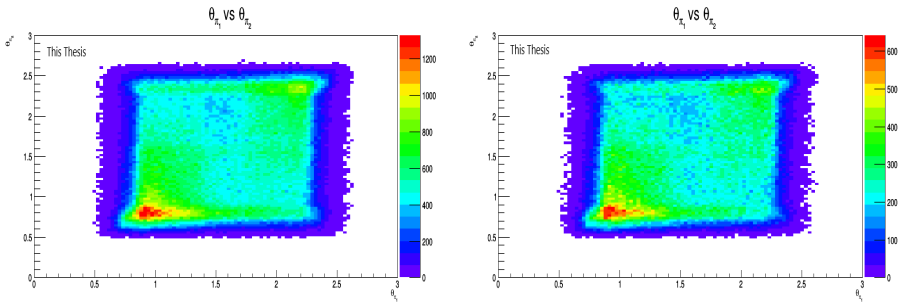

Figure 4.19: The left image shows the IM+PID+Pt+!V0 cut and the right image shows the IM+PID+Pt+!V0+!AD cut.

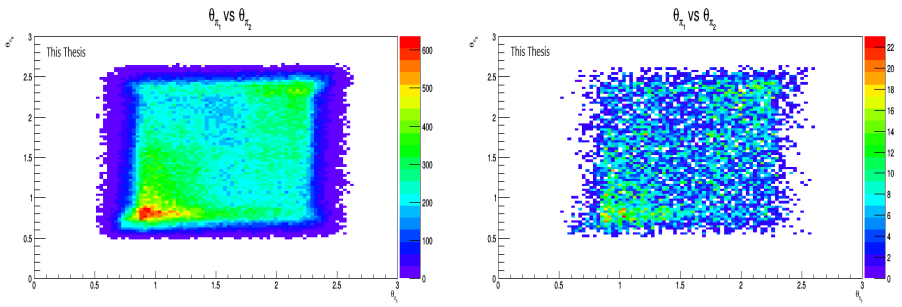

Figure 4.20: The left image shows the IM+PID+Pt+!V0+!AD+Vtx cut and the right image shows the IM+PID+Pt+!V0+!AD+Vtx+VtxChi2 cut.

Figures 4.21, 4.22, 4.23 and 4.24 show the graphs corresponding to the $\phi_{\pi_1} vs \phi_{\pi_2}$.

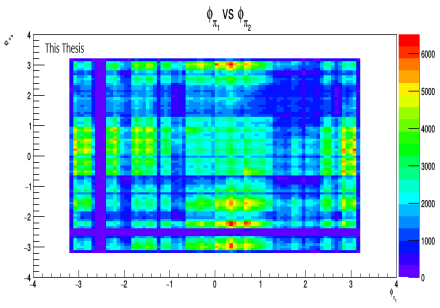

Figure 4.21: This figure shows the $\phi_{\pi_1} vs \phi_{\pi_2}$.

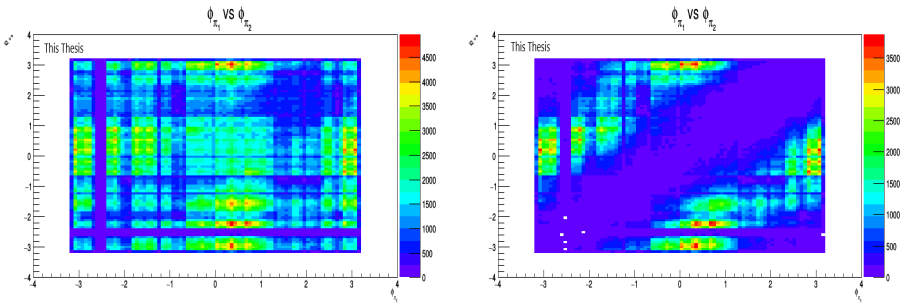

Figure 4.22: The left image shows the IM+PID cut and the right image shows the IM+PID+Pt cut.

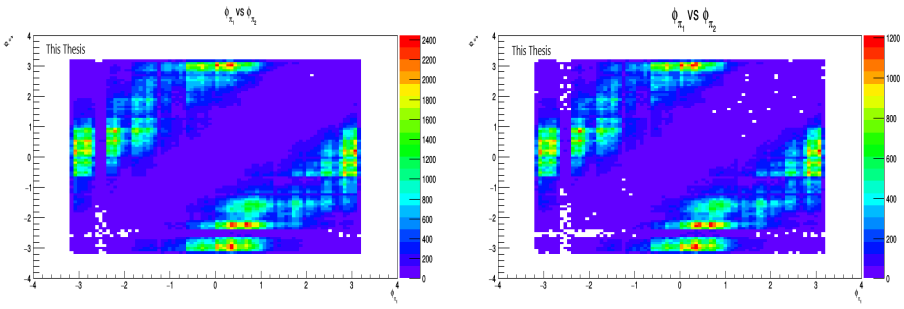

Figure 4.23: The left image shows the IM+PID+Pt+!V0 cut and the right image shows the IM+PID+Pt+!V0+!AD cut.

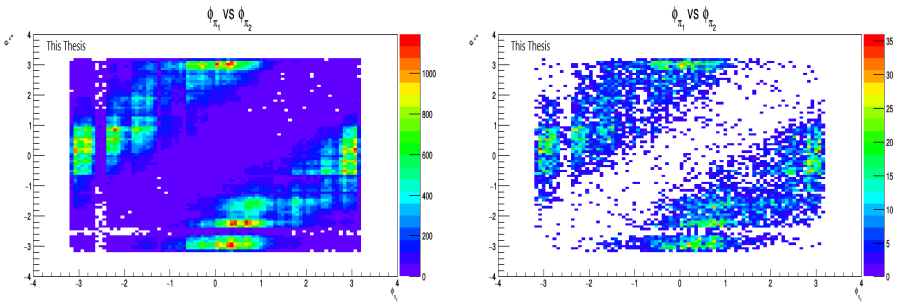

Figure 4.24: The left image shows the IM+PID+Pt+!V0+!AD+Vtx cut and the right image shows the IM+PID+Pt+!V0+!AD+Vtx+VtxChi2 cut.

On the other hand, you have the graphics corresponding to the V0 and AD offline decisions, the V0 and AD detectors offer the possibility to compute precise offline decisions flags [9]. These decisions are defined as follows:

- 0-1 (kEmpty): the detector is empty.
- 1-2 (kBB): the detector has a signal in the beam–beam time window.
- 2-3 (kBG): the detector has a signal in the beam–gas time window.
- 3-4 (kFake): the signal in the detector arrived at a time outside both the beam–beam and beam–gas windows.

Taking this fact into account, the following graphs 4.25, 4.26, 4.27, 4.28, 4.29, 4.30, 4.31, 4.32, 4.33, 4.34, 4.35 and 4.36 show the offline decisions with the respective cuts shown in table 4.1.

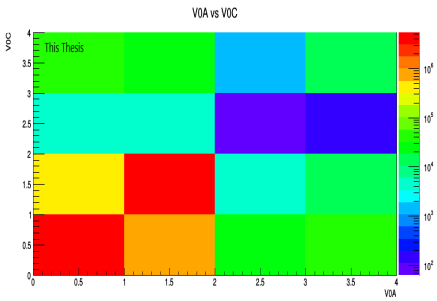

Figure 4.25: This figure shows the V0A vs V0C.

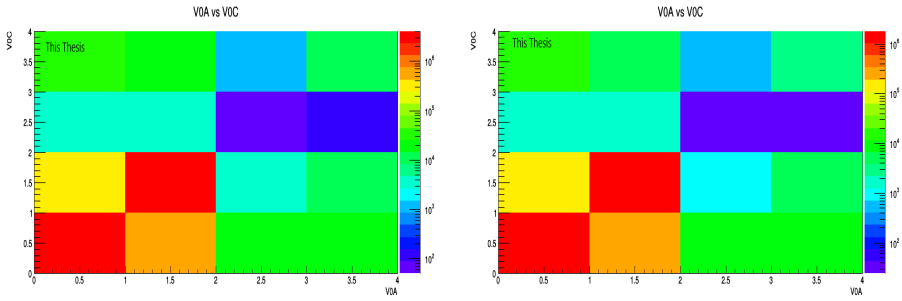

Figure 4.26: The left image shows the IM+PID cut and the right image shows the IM+PID+Pt cut.

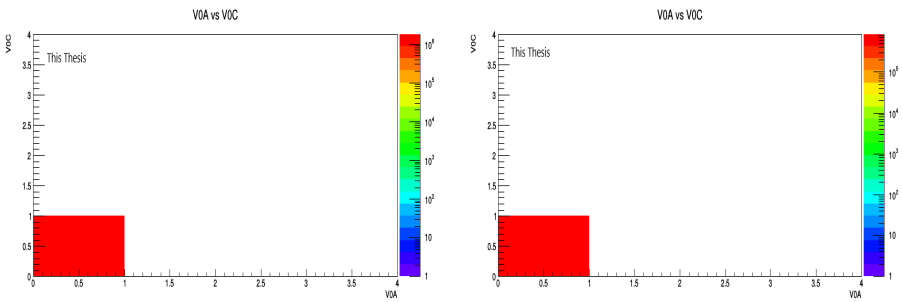

Figure 4.27: The left image shows the IM+PID+Pt+!V0 cut and the right image shows the IM+PID+Pt+!V0+!AD cut.

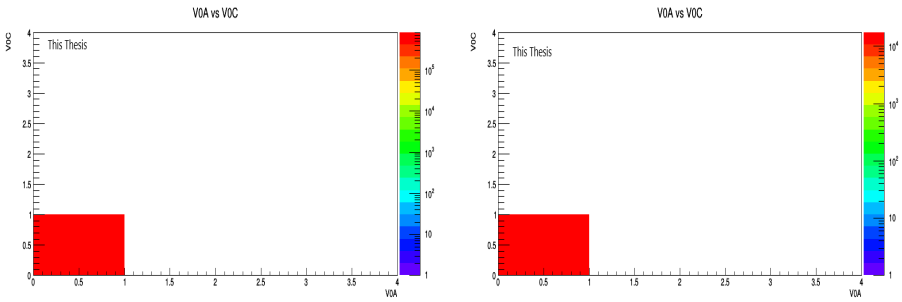

Figure 4.28: The left image shows the IM+PID+Pt+!V0+!AD+Vtx cut and the right image shows the IM+PID+Pt+!V0+!AD+Vtx+VtxChi2 cut.

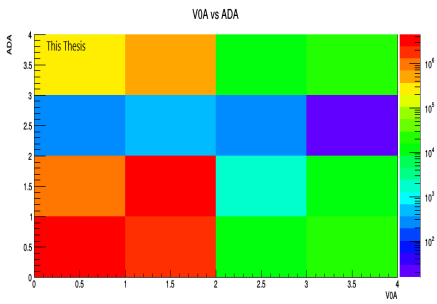

Figure 4.29: This figure shows the V0A vs ADA.

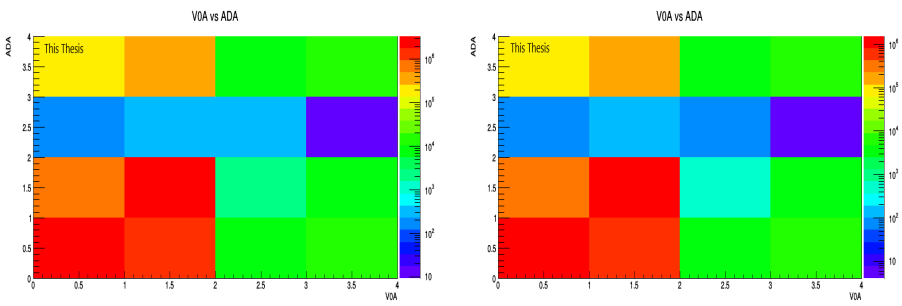

Figure 4.30: The left image shows the IM+PID cut and the right image shows the IM+PID+Pt cut.

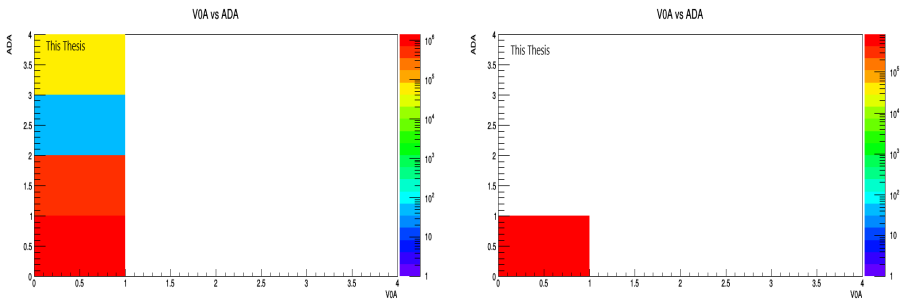

Figure 4.31: The left image shows the IM+PID+Pt+!V0 cut and the right image shows the IM+PID+Pt+!V0+!AD cut.

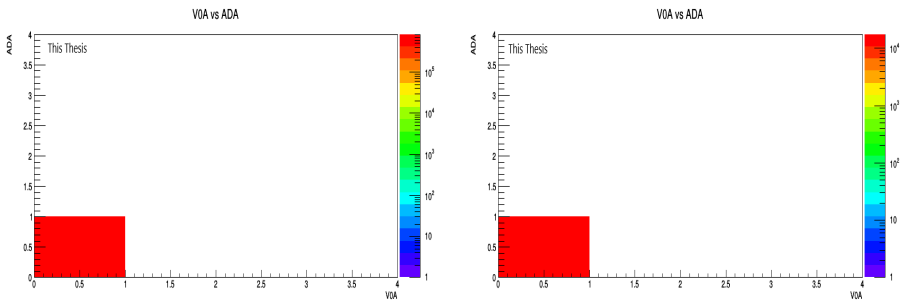

Figure 4.32: The left image shows the IM+PID+Pt+!V0+!AD+Vtx cut and the right image shows the IM+PID+Pt+!V0+!AD+Vtx+VtxChi2 cut.

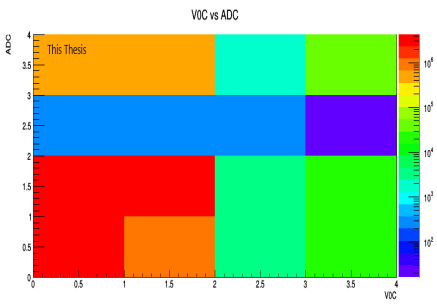

Figure 4.33: This figure shows the V0C vs ADC.

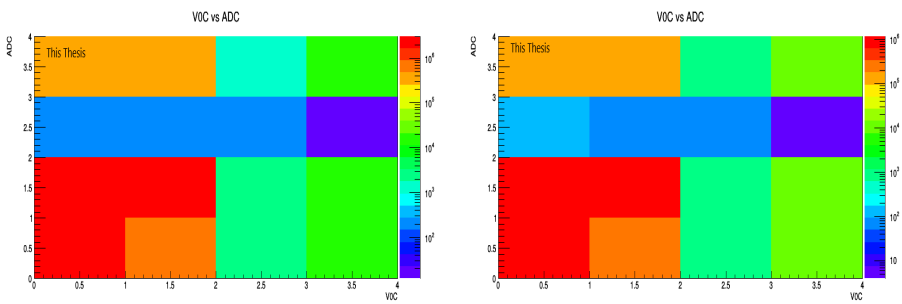

Figure 4.34: The left image shows the IM+PID cut and the right image shows the IM+PID+Pt cut.

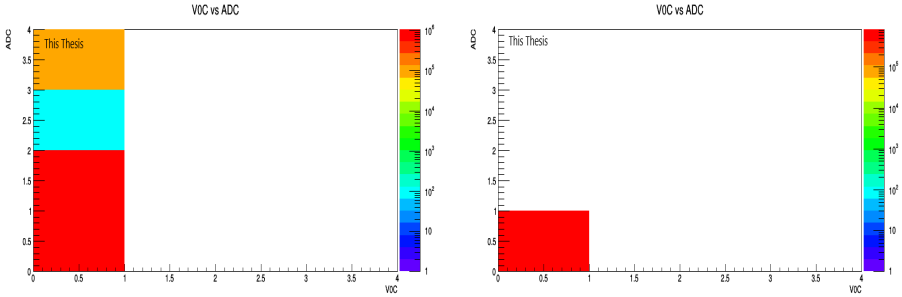

Figure 4.35: The left image shows the IM+PID+Pt+!V0 cut and the right image shows the IM+PID+Pt+!V0+!AD cut.

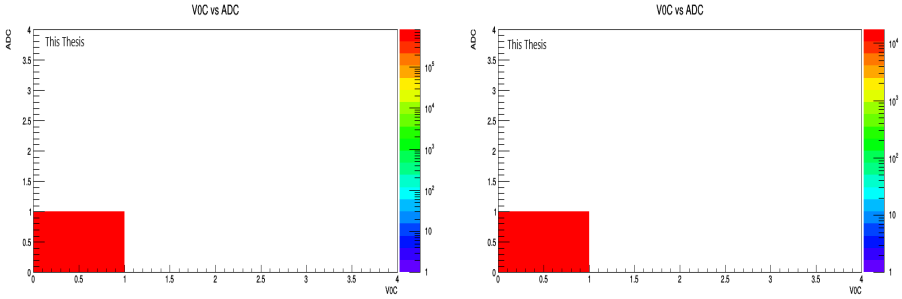

Figure 4.36: The left image shows the IM+PID+Pt+!V0+!AD+Vtx cut and the right image shows the IM+PID+Pt+!V0+!AD+Vtx+VtxChi2 cut.

It should be noted that in all the graphs previously shown the veto in the AD detector (!AD) does not cause a significant change within the data, which can be clearly seen in the invariant mass spectra shown.

4.3 Results for two pions

After the study and analysis of the previous cuts, the spectrum of the invariant mass without cuts was first obtained and the spectra of the same after making the cuts sequentially Fig 4.1 . It should be mentioned that from a decrease in the width of the bin of these cuts we were able to identify two very important spectra. These can be compared quantitatively with the histograms found, by means of the Bayesian Statistics, which is based on using the known data which in this case would be those obtained by the COMPASS experiment and by Taesoo Kim and Ju Hwan Kang, in order to make inferences in the unknown data or predictions, which would be the data obtained in the 10 longest runs, by means of the use of a parametric model. "In a basic

model we have a parameter of interest θ and some observed data D and we consider a joint probability distribution for both of them that shows how they are related: $p(\theta, D)$ "[1], which refers to the distribution of the predictions given the known data, which is expressed as follows

$$p(\theta|D) = \frac{p(\theta) \cdot p(D|\theta)}{p(D)} \tag{4.5}$$

Where

- $p(\theta)$ is the a priori distribution of *theta* which gives us *theta* information without the observed data information (D).
- $p(\theta|D)$ is the a posteriori distribution of *theta*, which, gives us the information of *theta* when we already know the observed data (D).

The first spectrum relates to the results of 2009 COMPASS [3] results and the cut corresponding to IM+PID+Pt+!V0+!AD+Vtx. It should be noted, however, that the structure of the spectrum similar to that of COMPASS can be seen slightly from the invariant mass graph without any cut.

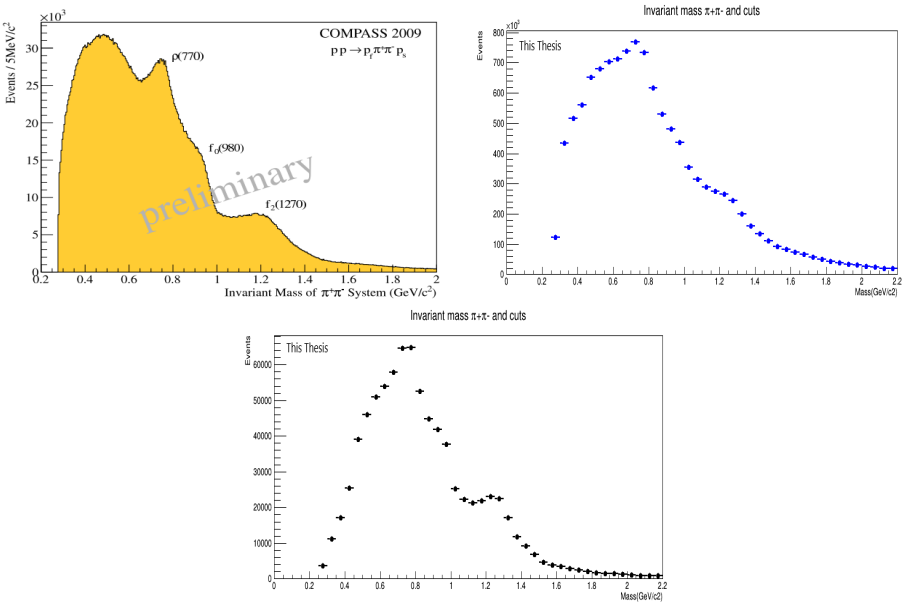

Figure 4.37: The image on the upper left corresponds to the graph obtained from the COMPASS experiment, the one on the upper right is the invariant mass spectrum without any cuts and the image in the centre alludes to the mass spectrum with the cuts IM + PID + Pt + !V0 + !AD + Vtx + VtxChi2.

Comparing the three spectra we can identify the similarities between the resonances of the graphs, among which we highlight the presence $\rho^0(770)$, $f_0(980)$ y $f_2(1270)$.

The second spectrum relates to the mass spectrum presented by Taesoo Kim and Ju Hwan Kang [11] and the cut corresponding to IM + PID + Pt + !V0 + !AD + Vtx + VtxChi2.

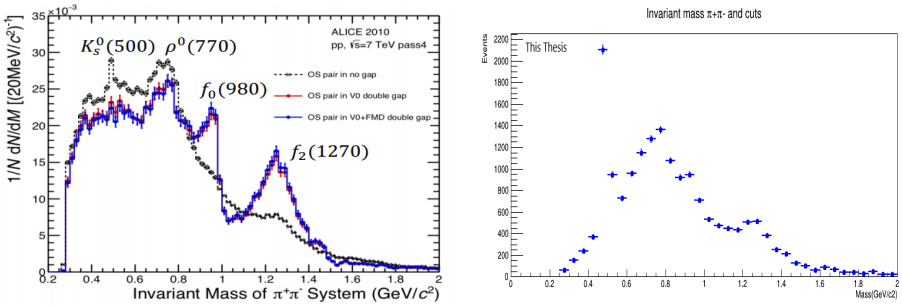

Figure 4.38: The image on the left corresponds to that obtained by Taesoo Kim and Ju Hwan Kang and the one on the right is the spectrum recorded from the 10 longest runs, with the cuts IM + PID + Pt + !V0 + !AD + Vtx + VtxChi2.

If we compare both spectra it is possible to identify the similarities between the two, in which we find the presence of $K_s^0(500)$, $\rho^0(770)$, $f_0(980)$ y $f_2(1270)$.

Among the resonances found we find that $f_0(980)$ and $f_2(1270)$ are considered as possible candidates for glueball, the resonances are usually defined as a phase change and can be distinguished in the invariant mass spectrum.

The $f_0(980)$ resonance is very close to the threshold and may fall to $\pi^+\pi^-$ or $K\bar{K}$. It should be noted that for this resonance "the mass is centered well above $\pi^+\pi^-$ threshold but for the decays into $K\bar{K}$, the mass is $K\bar{K}$ threshold. In this case, unitary and analyticity are used to extrapolate the KK threshold" [19].

On the other hand the $f_2(1270)$ resonance has a mass of 1285 MeV and was one of the first results shown by BNL in a reaction $p\bar{n} \rightarrow 2\pi^+\pi^-$.

Note that in addition to these two resonances there are others such as $f_0(500)$, $f_0(1370)$, $f_0(1500)$ and $f_0(1710)$ which are also considered glueball candidates [16].

4.4 Four pions analysis

The code to analyze the experimental data sample can be found in Appendix A. For the data analysis, the Aliroot software with ROOT version 5.34/30 was used.

4.4.1 Cuts or kinematical considerations

The same cuts as in the case of 2 pions analysis were applied for 4 pions analysis, the only difference between the cuts made for two pions and these is that the transverse moment (Pt) in this case is restricted by $Pt < 1.0$, that is

- PID is equal to $(\sigma_{\pi_1})^2 + (\sigma_{\pi_2})^2 < 4$
- Pt < 1.0
- !V0
- !AD
- $\mid Vtx \mid > 10$
- VtxChi2 > 100

Considering this change, we obtained the following table where each of the cuts made are presented with their respective entries

Cuts	Number of events
Invariant Mass (IM)	5744128
IM+PID	4234051
IM + PID + Pt	2161237
IM + PID + Pt +!V0	528640
IM + PID + Pt + !V0 + !AD	205137
IM + PID + Pt + !V0 + !AD + Vtx	202481
IM + PID + Pt + !V0 + !AD + Vtx + VtxChi2	2732

Table 4.2: Shows the cuts made to the invariant mass

For the case of 4 pions, the invariant mass spectra were plotted without cuts and with them

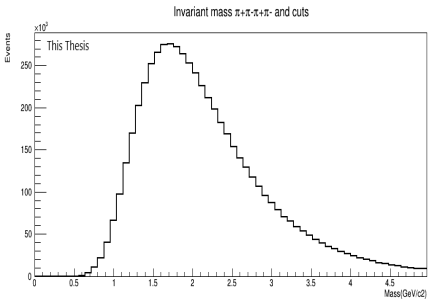

Figure 4.39: This figure shows the invariant mass.

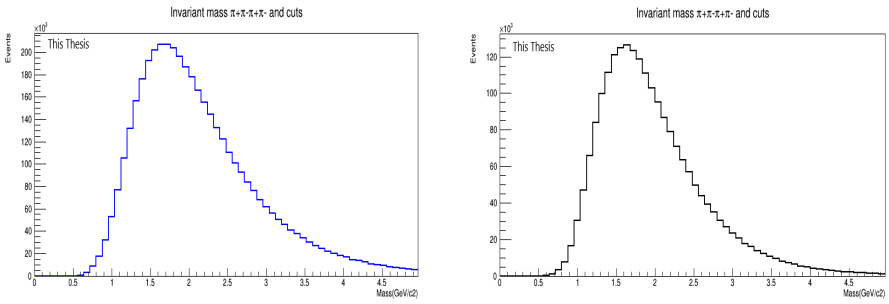

Figure 4.40: The left image shows the IM+PID cut and the right image shows the IM+PID+Pt cut.

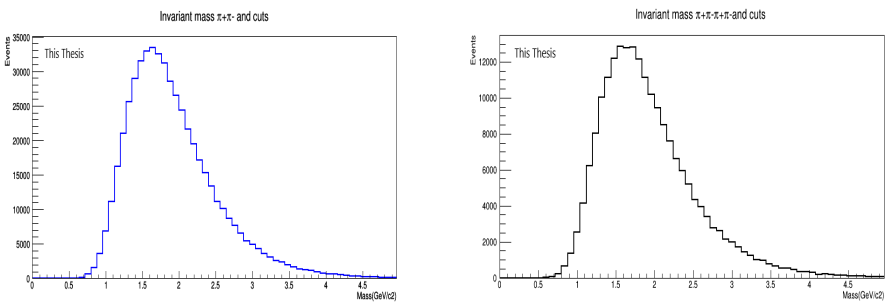

Figure 4.41: The left image shows the IM+PID+Pt+!V0 cut and the right image shows the IM+PID+Pt+!V0+!AD cut.

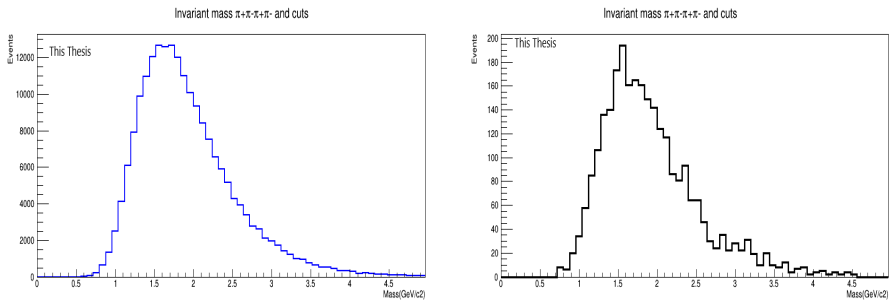

Figure 4.42: The left image shows the IM+PID+Pt+!V0+!AD+Vtx cut and the right image shows the IM+PID+Pt+!V0+!AD+Vtx+VtxChi2 cut.

4.5 Results for four pions

By making a decrease in the width of the bin of these cuts we were able to identify a mass spectrum very similar to that obtained by the STAR detector, with the difference that the STAR experiment carried out the study for the production of 4 pions by means of heavy ions in ultraperipheral collisions and we did this analysis for proton-proton collisions in diffractive processes.

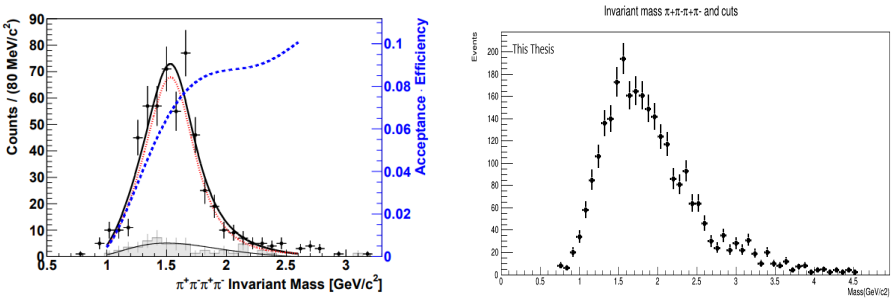

Figure 4.43: The left side shows the spectra obtained by the STAR [2] experiment and the right side shows the spectrum obtained from the ten longest runs.

It should be noted that the image on the right side represents the invariant mass with the following cuts IM+PID+Pt+!V0+!AD+Vtx+VtxChi2. From both spectra we can notice the clear similarity that exists around the resonance presented which is presented in approximately 1.5 GeV.

Chapter 5

Summary and Reflections

Data from the ten longest runs in the years 2017 and 2018 were analyzed with the triggers CCUP25-B-SPD1-CENTNOTRD and CCUP13-B-SPD1-CENTNOTRD, to study the central production of 2 and 4 pions in diffractive processes.

In this work, it is necessary to express that good results were obtained from both studies, since for the case of 2 pions, the graphs for both triggers were very similar, since very similar spectra were recorded in all the cuts. And it is from these that structures could be identified that could correspond to $K_s^0(500)$, $\rho^0(770)$, $f_0(980)$ y $f_2(1270)$, which are reported by COMPASS and Taesoo Kim and Ju Hwan Kang .

On the other hand, for the case of 4 pions, the graphs of both triggers were also very similar before the invariant mass structures. It should be noted that the last cut made in this sample is of great importance since it is very similar to the one obtained by the STAR detector with the difference that this detector recorded the mass spectrum for 4 pions by means of ultra-peripheral collisions and the spectrum that we obtained from the 10 longest runs was obtained from diffractive processes, This is the first evidence of 4 pion production un central diffractive events with proton-proton collisions ar 13 TeV.

As a continuation of this work, it is proposed to repeat this same study but for all the runs registered in the years 2017 and 2018 with the triggers CCUP25-B-SPD1-CENTNOTRD and CCUP13-B-SPD1-CENTNOTRD.

Bibliography

[1] *Tema 2: Modelos Básicos de Estadística Bayesiana.*

[2] Abelev, B. . *Observation of $\pi + \pi - \pi + \pi-$ Photoproduction in Ultra-Peripheral Heavy Ion Collisions at $\sqrt{s_{NN}} = 200$ GeV at the STAR Detector.* arxiv.org/pdf/0912.0604.v2 . p.9, 2013.

[3] Austregesilo, A. *Central Production of Two-Pseudoscalar Final States at COMPASS.* arxiv.org/pdf/1310.3190.v1. p.4, 2013.

[4] Barone, V. y Predazzi, E. *High-Energy Particle Driffraction.* Springer, 2002.

[5] Collaboration, A. *Particle identification in ALICE: a Bayesian approach.* arXiv:1602.01392v2, 2016.

[6] collaboration, T. A. *Measurement of inelastic, single- and double-diffraction cross sections in proton-proton collisions at the LHC with ALICE.* THE EUROPEAN PHYSICAL JOURNAL C, 2013.

[7] Daw, E. *Rapidity and Pseudorapidity.* 2012.

[8] Griffiths, D. *And introduction to elementary particle physics.* WILEY-VCH, 2004.

[9] Horak, D., C. G. *Coherent ρ^0 vector meson photoproduction at midrapidity in Xe-Xe collisions at $\sqrt{s_{NN}} = 5.44$ TeV.* European Organization Nuclear Research, 2020.

[10] Jackson, D. *Classical Electrodynamics.* Berkeley: JOHN WILEY SONS, INC., 1998.

[11] Kim, T., and Hwan K., J. *Partial wave analysis of centrally produced $\pi + \pi-$ system in p-p collisions at $\sqrt{s} = 7$ TeV.* URL: https://home.cern/science/experiments/alice, 2017.

[12] Klempt, E., and Zaitsev, A. *Glueballs, Hybrids, Multiquarks. Experimental facts versus QCD inspired concepts.* 2007.

[13] Knospe, A. *Recent hadronic resonance measurements at ALICE.* arXiv:1610.09529v1, 2016.

[14] Lepora, N. *Modelling Rho-Pion-Electromagnetic Interactions with an Effective Weinberg-Salam Theory.* Department of Applied Mathematics and Theoretical Physics, Cambridge University, England, 1999.

[15] Lichard, P., and Juran, J. *Four-charged-pion decay of 0(770) and the a1 Lagrangian.* arXiv:hep-ph/0601234 v1, 2006.

[16] Ochs, W. *The Status of Glueballs.* Max-Planck-Institut fur Physik, Werner-Heisenberg-Institut, 2013.

[17] Revol, J. *Diffractive Physics at the CERN Large Hadron Collider.* Nuclear Physics A, 2011.

[18] science, C. A. *ALICE.* home.cern/science/experiments/alice, Recuperado: 19/05/2020.

[19] Toki, W. *Search for Glueballs.* Department oh Physics, Colorado State University, 1996.

[20] Trzebinski, M. *Study of QCD and Diffraction with the ATLAS detector at the LHC.* Thesis,Universite Paris-Sud, 2013.

[21] Villatoro, A. *Detection and discrimation of diffractive events with ALICE-LHC at CERN. Tesis Doctoral.* Benemérita Universidad Autónoma de Puebla.Puebla, 2019.

[22] y Tecnológica para ALICE LHC, R. M. C. *¿Qué es el experimento ALICE?* http://alice.nucleares.unam.mx/experimento$_alice$, 2015.

Appendix A

Codes

A.1 Two pions

void analisiscor2()

//TFile* f = new TFile("AnalysisResults$_0 a.root$");

// TFile* f = new TFile("AnalysisResults1.root");

TFile* f = new TFile("18l-ccup13-2pi.root");

Int$_t RunNum_T = 0$;

UShort$_t BunchCrossNumber_T = 0$;

UInt$_t OrbitNumber_T = 0$;

UInt$_t PeriodNumber_T = 0$;

Bool$_t LikeSign_T$;

Float$_t Mass_T = 0$;

Float$_t Pt_T = 0$;

Float$_t Rapidity_T = 0$;

Float$_t Mass_T P = 0; //added$

Float$_t Pt_T P = 0; //added$

Float$_t Rapidity_T P = 0; //added$

Float$_t Mass_T K = 0; //added$

Float$_t Pt_T K = 0; //added$

Float$_t Rapidity_T K = 0; //added$

$\mathrm{Int}_t V0Adecision_T = 0;$

$\mathrm{Int}_t V0Cdecision_T = 0;$

$\mathrm{Int}_t ADAdecision_T = 0;$

$\mathrm{Int}_t ADCdecision_T = 0;$

$\mathrm{Bool}_t UBAfired_T = 0;$

$\mathrm{Bool}_t UBCfired_T = 0;$

$\mathrm{Float}_t ZNAenergy_T = 0;$

$\mathrm{Float}_t ZNCenergy_T = 0;$

$\mathrm{Float}_t ZPAenergy_T = 0;$

$\mathrm{Float}_t ZPCenergy_T = 0;$

$\mathrm{Float}_t ZDCAtime_T[4];$

$\mathrm{Float}_t ZDCCtime_T[4];$

$\mathrm{Float}_t PIDTPCPion_T[2];$

$//\mathrm{Float}_t PIDTPCElectron_T[2];$

$\mathrm{Float}_t PIDTPCKaon_T[2]; //added$

$\mathrm{Float}_t PIDTPCProton_T[2]; //added$

$\mathrm{Float}_t PIDTPCMuon_T[2]; //added$

$\mathrm{Int}_t TPCsignal_T[2];$

$\mathrm{Float}_t TrackP_T[2];$

$\mathrm{Float}_t Vertex_T[3];$

$\mathrm{Int}_t VtxContrib_T = 0;$

$\mathrm{Float}_t VtxChi2_T, VtxNDF_T = 0;$

$\mathrm{Float}_t SpdVertex_T[3];$

$\mathrm{Int}_t SpdVtxContrib_T = 0;$

$\mathrm{Int}_t Ntracklets_T = 0;$

$\mathrm{Float}_t Phi_T = 0;$

$\mathrm{Float}_t Phi_T P = 0; //added$

$\mathrm{Float}_t Phi_T K = 0; //added$

$\mathrm{Float}_t TrackEta_T[2];$

$\mathrm{Float}_t TrackPhi_T[2];$

$\mathrm{Float}_t TrackPx_T[2];$

$\mathrm{Float}_t TrackPy_T[2];$

$\mathrm{Float}_t TrackPz_T[2];$

$\mathrm{Bool}_t ChipCut_T = 0;$

$\mathrm{Int}_t ITSModuleInner_T[2];$

$\mathrm{Int}_t ITSModuleOuter_T[2];$

RhoTree→SetBranchAddress("RunNum_T", $RunNum_T$);

RhoTree→SetBranchAddress("$\mathrm{PeriodNumber}_T$", $PeriodNumber_T$);

RhoTree→SetBranchAddress("$\mathrm{OrbitNumber}_T$", $OrbitNumber_T$);

RhoTree→SetBranchAddress("$\mathrm{BunchCrossNumber}_T$", $BunchCrossNumber_T$);

RhoTree→SetBranchAddress("$\mathrm{LikeSign}_T$", $LikeSign_T$);

RhoTree→SetBranchAddress("Mass_T", $Mass_T$);

RhoTree→SetBranchAddress("Pt_T", Pt_T);

RhoTree→SetBranchAddress("$\mathrm{Rapidity}_T$", $Rapidity_T$);

RhoTree→SetBranchAddress("Phi_T", Phi_T);

RhoTree→SetBranchAddress("$\mathrm{Mass}_T P$", $Mass_T P$); //*added*

RhoTree→SetBranchAddress("$\mathrm{Pt}_T P$", $Pt_T P$); //*added*

RhoTree→SetBranchAddress("$\mathrm{Rapidity}_T P$", $Rapidity_T P$); //*added*

RhoTree→SetBranchAddress("$\mathrm{Phi}_T P$", $Phi_T P$); //*added*

RhoTree→SetBranchAddress("$\mathrm{Mass}_T K$", $Mass_T K$); //*added*

RhoTree→SetBranchAddress("$\mathrm{Pt}_T K$", $Pt_T K$); //*added*

RhoTree→SetBranchAddress("$\mathrm{Rapidity}_T K$", $Rapidity_T K$); //*added*

RhoTree→SetBranchAddress("$\mathrm{Phi}_T K$", $Phi_T K$); //*added*

RhoTree→SetBranchAddress("$\mathrm{ZNAenergy}_T$", $ZNAenergy_T$);

RhoTree→SetBranchAddress("$\mathrm{ZNCenergy}_T$", $ZNCenergy_T$);

RhoTree→SetBranchAddress("$\mathrm{ZPAenergy}_T$", $ZPAenergy_T$);

RhoTree→SetBranchAddress("$\mathrm{ZPCenergy}_T$", $ZPCenergy_T$);

RhoTree→SetBranchAddress("$\mathrm{ZDCAtime}_T$", $ZDCAtime_T$);

RhoTree→SetBranchAddress("ZDCCtime$_T$", $ZDCCtime_T$);

RhoTree→SetBranchAddress("PIDTPCPion$_T$", $PIDTPCPion_T$);

RhoTree→SetBranchAddress("PIDTPCProton$_T$", $PIDTPCProton_T$); //*added*

RhoTree→SetBranchAddress("PIDTPCKaon$_T$", $PIDTPCKaon_T$); //*added*

RhoTree→SetBranchAddress("TPCsignal$_T$", $TPCsignal_T$);

RhoTree→SetBranchAddress("TrackP$_T$", $TrackP_T$);

RhoTree→SetBranchAddress("TrackEta$_T$", $TrackEta_T$);

RhoTree→SetBranchAddress("TrackPhi$_T$", $TrackPhi_T$);

RhoTree→SetBranchAddress("TrackPx$_T$", $TrackPx_T$);

RhoTree→SetBranchAddress("TrackPy$_T$", $TrackPy_T$);

RhoTree→SetBranchAddress("TrackPz$_T$", $TrackPz_T$);

RhoTree→SetBranchAddress("VtxX$_T$", $Vertex_T[0]$);

RhoTree→SetBranchAddress("VtxY$_T$", $Vertex_T[1]$);

RhoTree→SetBranchAddress("VtxZ$_T$", $Vertex_T[2]$);

RhoTree→SetBranchAddress("VtxContrib$_T$", $VtxContrib_T$);

RhoTree→SetBranchAddress("VtxChi2$_T$", $VtxChi2_T$);

RhoTree→SetBranchAddress("VtxNDF$_T$", $VtxNDF_T$);

RhoTree→SetBranchAddress("SpdVtxX$_T$", $SpdVertex_T[0]$);

RhoTree→SetBranchAddress("SpdVtxY$_T$", $SpdVertex_T[1]$);

RhoTree→SetBranchAddress("SpdVtxZ$_T$", $SpdVertex_T[2]$);

RhoTree→SetBranchAddress("SpdVtxContrib$_T$", $SpdVtxContrib_T$);

RhoTree→SetBranchAddress("V0Adecision$_T$", $V0Adecision_T$);

RhoTree→SetBranchAddress("V0Cdecision$_T$", $V0Cdecision_T$);

RhoTree→SetBranchAddress("ADAdecision$_T$", $ADAdecision_T$);

RhoTree→SetBranchAddress("ADCdecision$_T$", $ADCdecision_T$);

RhoTree→SetBranchAddress("UBAfired$_T$", $UBAfired_T$);

RhoTree→SetBranchAddress("UBCfired$_T$", $UBCfired_T$);

RhoTree→SetBranchAddress("Ntracklets$_T$", $Ntracklets_T$);

RhoTree→SetBranchAddress("ChipCut$_T$", $ChipCut_T$);

```
TH1D *masapi0 = new TH1D("masapi0","Invariant mass pi+pi- and cuts; Mass(GeV/c2);
Events",200,0,10);
TH1D *masapi1 = new TH1D("masapi1","Invariant mass pi+pi- and cuts; Mass(GeV/c2);
Events",200,0,10);
TH1D *masapi2 = new TH1D("masapi2","Invariant mass pi+pi- and cuts; Mass(GeV/c2);
Events",200,0,10);
TH1D *masapi3 = new TH1D("masapi3","Invariant mass pi+pi- and cuts; Mass(GeV/c2);
Events",200,0,10);
TH1D *masapi4 = new TH1D("masapi4","Invariant mass pi+pi- and cuts; Mass(GeV/c2);
Events",200,0,10);
TH1D *masapi5 = new TH1D("masapi5","Invariant mass pi+pi- and cuts; Mass(GeV/c2);
Events",200,0,10);
TH1D *masapi6 = new TH1D("masapi6","Invariant mass pi+pi- and cuts; Mass(GeV/c2);
Events",200,0,10);
TH2D *MPtpi0= new TH2D("MPtpi0", "Invariant Mass vs Pt; Mass (GeV/c2); Pt
(GeV/c)", 100, 0, 4, 100, 0, 3);
TH2D *MPtpi1= new TH2D("MPtpi1", "Invariant Mass vs Pt; Mass (GeV/c2); Pt
(GeV/c)", 100, 0, 4, 100, 0, 3);
TH2D *MPtpi2= new TH2D("MPtpi2", "Invariant Mass vs Pt; Mass (GeV/c2); Pt
(GeV/c)", 100, 0, 4, 100, 0, 0.51);
TH2D *MPtpi3= new TH2D("MPtpi3", "Invariant Mass vs Pt; Mass (GeV/c2); Pt
(GeV/c)", 100, 0, 4, 100, 0, 0.51);
TH2D *MPtpi4= new TH2D("MPtpi4", "Invariant Mass vs Pt; Mass (GeV/c2); Pt
(GeV/c)", 100, 0, 4, 100, 0, 0.51);
TH2D *MPtpi5= new TH2D("MPtpi5", "Invariant Mass vs Pt; Mass (GeV/c2); Pt
(GeV/c)", 100, 0, 4, 100, 0, 0.51);
TH2D *MPtpi6= new TH2D("MPtpi6", "Invariant Mass vs Pt; Mass (GeV/c2); Pt
(GeV/c)", 100, 0, 4, 100, 0, 0.51);
TH2F *V00 = new TH2F("V00","V0A vs V0C; V0A;V0C",4,0,4,4,0,4);
```

```
TH2F *V01 = new TH2F("V01","V0A vs V0C; V0A;V0C",4,0,4,4,0,4);
TH2F *V02 = new TH2F("V02","V0A vs V0C; V0A;V0C",4,0,4,4,0,4);
TH2F *V03 = new TH2F("V03","V0A vs V0C; V0A;V0C",4,0,4,4,0,4);
TH2F *V04 = new TH2F("V04","V0A vs V0C; V0A;V0C",4,0,4,4,0,4);
TH2F *V05 = new TH2F("V05","V0A vs V0C; V0A;V0C",4,0,4,4,0,4);
TH2F *V06 = new TH2F("V06","V0A vs V0C; V0A;V0C",4,0,4,4,0,4);
TH2F *V0AADA0 = new TH2F("V0AADA0","V0A vs ADA; V0A; ADA",4,0,4,4,0,4);
TH2F *V0AADA1 = new TH2F("V0AADA1","V0A vs ADA; V0A; ADA",4,0,4,4,0,4);
TH2F *V0AADA2 = new TH2F("V0AADA2","V0A vs ADA; V0A; ADA",4,0,4,4,0,4);
TH2F *V0AADA3 = new TH2F("V0AADA3","V0A vs ADA; V0A; ADA",4,0,4,4,0,4);
TH2F *V0AADA4 = new TH2F("V0AADA4","V0A vs ADA; V0A; ADA",4,0,4,4,0,4);
TH2F *V0AADA5 = new TH2F("V0AADA5","V0A vs ADA; V0A; ADA",4,0,4,4,0,4);
TH2F *V0AADA6 = new TH2F("V0AADA6","V0A vs ADA; V0A; ADA",4,0,4,4,0,4);
TH2F *V0CADC0= new TH2F("V0CADC0","V0C vs ADC; V0C; ADC",4,0,4,4,0,4);
TH2F *V0CADC1= new TH2F("V0CADC1","V0C vs ADC; V0C; ADC",4,0,4,4,0,4);
TH2F *V0CADC2= new TH2F("V0CADC2","V0C vs ADC; V0C; ADC",4,0,4,4,0,4);
TH2F *V0CADC3= new TH2F("V0CADC3","V0C vs ADC; V0C; ADC",4,0,4,4,0,4);
TH2F *V0CADC4= new TH2F("V0CADC4","V0C vs ADC; V0C; ADC",4,0,4,4,0,4);
TH2F *V0CADC5= new TH2F("V0CADC5","V0C vs ADC; V0C; ADC",4,0,4,4,0,4);
TH2F *V0CADC6= new TH2F("V0CADC6","V0C vs ADC; V0C; ADC",4,0,4,4,0,4);
TH2F *hPIDtrk0trk0 = new TH2F("hPIDtrk0trk0","PIDtrack0 vs PIDtrack1; PID-
track0; PIDtrack1",100,-4,4,100,-4,4);
TH2F *hPIDtrk0trk1 = new TH2F("hPIDtrk0trk1","PIDtrack0 vs PIDtrack1; PID-
track0; PIDtrack1",100,-4,4,100,-4,4);
TH2F *hPIDtrk0trk2 = new TH2F("hPIDtrk0trk2","PIDtrack0 vs PIDtrack1; PID-
track0; PIDtrack1",100,-4,4,100,-4,4);
TH2F *hPIDtrk0trk3 = new TH2F("hPIDtrk0trk3","PIDtrack0 vs PIDtrack1; PID-
track0; PIDtrack1",100,-4,4,100,-4,4);
TH2F *hPIDtrk0trk4 = new TH2F("hPIDtrk0trk4","PIDtrack0 vs PIDtrack1; PID-
```

track0; PIDtrack1”,100,-4,4,100,-4,4);

TH2F *hPIDtrk0trk5 = new TH2F(”hPIDtrk0trk5”,”PIDtrack0 vs PIDtrack1; PID-track0; PIDtrack1”,100,-4,4,100,-4,4);

TH2F *hPIDtrk0trk6 = new TH2F(”hPIDtrk0trk6”,”PIDtrack0 vs PIDtrack1; PID-track0; PIDtrack1”,100,-4,4,100,-4,4);

TH2F *PhiPhipi0 = new TH2F(”PhiPhipi0”, ”Phi 1 vs Phi 2; Phi 1; Phi 2”, 100, -4, 4, 100, -4,4);

TH2F *PhiPhipi1 = new TH2F(”PhiPhipi1”, ”Phi 1 vs Phi 2; Phi 1; Phi 2”, 100, -4, 4, 100, -4,4);

TH2F *PhiPhipi2 = new TH2F(”PhiPhipi2”, ”Phi 1 vs Phi 2; Phi 1; Phi 2”, 100, -4, 4, 100, -4,4);

TH2F *PhiPhipi3 = new TH2F(”PhiPhipi3”, ”Phi 1 vs Phi 2; Phi 1; Phi 2”, 100, -4, 4, 100, -4,4);

TH2F *PhiPhipi4 = new TH2F(”PhiPhipi4”, ”Phi 1 vs Phi 2; Phi 1; Phi 2”, 100, -4, 4, 100, -4,4);

TH2F *PhiPhipi5 = new TH2F(”PhiPhipi5”, ”Phi 1 vs Phi 2; Phi 1; Phi 2”, 100, -4, 4, 100, -4,4);

TH2F *PhiPhipi6 = new TH2F(”PhiPhipi6”, ”Phi 1 vs Phi 2; Phi 1; Phi 2”, 100, -4, 4, 100, -4,4);

TH2F *Thetapi0 = new TH2F(”Thetapi0”, ”Theta 1 vs Theta 2; Theta 1; Theta 2”, 100, 0, 3, 100, 0, 3);

TH2F *Thetapi1 = new TH2F(”Thetapi1”, ”Theta 1 vs Theta 2; Theta 1; Theta 2”, 100, 0, 3, 100, 0, 3);

TH2F *Thetapi2 = new TH2F(”Thetapi2”, ”Theta 1 vs Theta 2; Theta 1; Theta 2”, 100, 0, 3, 100, 0, 3);

TH2F *Thetapi3 = new TH2F(”Thetapi3”, ”Theta 1 vs Theta 2; Theta 1; Theta 2”, 100, 0, 3, 100, 0, 3);

TH2F *Thetapi4 = new TH2F(”Thetapi4”, ”Theta 1 vs Theta 2; Theta 1; Theta 2”, 100, 0, 3, 100, 0, 3);

TH2F *Thetapi5 = new TH2F("Thetapi5", "Theta 1 vs Theta 2; Theta 1; Theta 2", 100, 0, 3, 100, 0, 3);

TH2F *Thetapi6 = new TH2F("Thetapi6", "Theta 1 vs Theta 2; Theta 1; Theta 2", 100, 0, 3, 100, 0, 3);

TH2F *Pt1Pt2pi0 = new TH2F("Pt1Pt2pi0", "Pt 1 VS Pt 2 ; Pt 1 (GeV/c); Pt 2 (GeV/c)", 100, 0, 4, 100, 0, 4);

TH2F *Pt1Pt2pi1 = new TH2F("Pt1Pt2pi1", "Pt 1 VS Pt 2 ; Pt 1 (GeV/c); Pt 2 (GeV/c)", 100, 0, 4, 100, 0, 4);

TH2F *Pt1Pt2pi2 = new TH2F("Pt1Pt2pi2", "Pt 1 VS Pt 2 ; Pt 1 (GeV/c); Pt 2 (GeV/c)", 100, 0, 4, 100, 0, 4);

TH2F *Pt1Pt2pi3 = new TH2F("Pt1Pt2pi3", "Pt 1 VS Pt 2 ; Pt 1 (GeV/c); Pt 2 (GeV/c)", 100, 0, 4, 100, 0, 4);

TH2F *Pt1Pt2pi4 = new TH2F("Pt1Pt2pi4", "Pt 1 VS Pt 2 ; Pt 1 (GeV/c); Pt 2 (GeV/c)", 100, 0, 4, 100, 0, 4);

TH2F *Pt1Pt2pi5 = new TH2F("Pt1Pt2pi5", "Pt 1 VS Pt 2 ; Pt 1 (GeV/c); Pt 2 (GeV/c)", 100, 0, 4, 100, 0, 4);

TH2F *Pt1Pt2pi6 = new TH2F("Pt1Pt2pi6", "Pt 1 VS Pt 2 ; Pt 1 (GeV/c); Pt 2 (GeV/c)", 100, 0, 4, 100, 0, 4);

for (Int$_t ev = 0; ev < RhoTree$→GetEntries();ev++)

RhoTree→GetEntry(ev);

//piones

TLorentzVector u1;

u1.SetPtEtaPhiM(sqrt(TrackPx$_T$[0]**2+$TrackPy_T$[0]**2), $TrackEta_T$[0], $TrackPhi_T$[0], 0.13957061);

TLorentzVector u2;

u2.SetPtEtaPhiM(sqrt(TrackPx$_T$[1]**2+$TrackPy_T$[1]**2), $TrackEta_T$[1], $TrackPhi_T$[1], 0.13957061);

TLorentzVector u3=u1+u2;

if(LikeSign$_T$ == 0)

masapi0→Fill(Mass$_T$);

MPtpi0→Fill(Mass$_T$, Pt_T);

V00→Fill(V0Adecision$_T$, $V0Cdecision_T$);

V0AADA0→Fill(V0Adecision$_T$, $ADAdecision_T$);

V0CADC0→Fill(V0Cdecision$_T$, $ADCdecision_T$);

hPIDtrk0trk0→Fill(PIDTPCPion$_T$[0], $PIDTPCPion_T$[1]);→ PhiPhipi0→Fill(u1.Phi(),u2.Phi());

Thetapi0→Fill(u1.Theta(),u2.Theta());

Pt1Pt2pi0→Fill(u1.Pt(),u2.Pt());

if(PIDTPCPion$_T$[0] $**2 + PIDTPCPion_T$[1] $**2 < 4$)

masapi1→Fill(Mass$_T$);

MPtpi1→Fill(Mass$_T$, Pt_T);

V01→Fill(V0Adecision$_T$, $V0Cdecision_T$);

V0AADA1→Fill(V0Adecision$_T$, $ADAdecision_T$);

V0CADC1→Fill(V0Cdecision$_T$, $ADCdecision_T$);

hPIDtrk0trk1→Fill(PIDTPCPion$_T$[0], $PIDTPCPion_T$[1]);

PhiPhipi1→Fill(u1.Phi(),u2.Phi());

Thetapi1→Fill(u1.Theta(),u2.Theta());

Pt1Pt2pi1→Fill(u1.Pt(),u2.Pt());

if(Pt$_T$ < 0.5)

masapi2→Fill(Mass$_T$);

MPtpi2→Fill(Mass$_T$, Pt_T);

V02→Fill(V0Adecision$_T$, $V0Cdecision_T$);

V0AADA2→Fill(V0Adecision$_T$, $ADAdecision_T$);

V0CADC2→Fill(V0Cdecision$_T$, $ADCdecision_T$);

hPIDtrk0trk2→Fill(PIDTPCPion$_T$[0], $PIDTPCPion_T$[1]);

PhiPhipi2→Fill(u1.Phi(),u2.Phi());

Thetapi2→Fill(u1.Theta(),u2.Theta());

Pt1Pt2pi2→Fill(u1.Pt(),u2.Pt());

if(V0Adecision$_T$ $== 0V0Cdecision_T == 0$)

masapi3→Fill(Mass$_T$);

MPtpi3→Fill(Mass$_T$, Pt_T);

V03→Fill(V0Adecision$_T$, $V0Cdecision_T$);

V0AADA3→Fill(V0Adecision$_T$, $ADAdecision_T$);

V0CADC3→Fill(V0Cdecision$_T$, $ADCdecision_T$);

hPIDtrk0trk3→Fill(PIDTPCPion$_T$[0], $PIDTPCPion_T$[1]);

PhiPhipi3→Fill(u1.Phi(),u2.Phi());

Thetapi3→Fill(u1.Theta(),u2.Theta());

Pt1Pt2pi3→Fill(u1.Pt(),u2.Pt());

if(ADAdecision$_T$ == 0$ADCdecision_T$ == 0)

masapi4→Fill(Mass$_T$);

MPtpi4→Fill(Mass$_T$, Pt_T);

V04→Fill(V0Adecision$_T$, $V0Cdecision_T$);

V0AADA4→Fill(V0Adecision$_T$, $ADAdecision_T$);

V0CADC4→Fill(V0Cdecision$_T$, $ADCdecision_T$);

hPIDtrk0trk4→Fill(PIDTPCPion$_T$[0], $PIDTPCPion_T$[1]);

PhiPhipi4→Fill(u1.Phi(),u2.Phi());

Thetapi4→Fill(u1.Theta(),u2.Theta());

Pt1Pt2pi4→Fill(u1.Pt(),u2.Pt());

if(Vertex$_T$[2] $< 10Vertex_T[2] > -10$)

masapi5→Fill(Mass$_T$);

MPtpi5→ill(Mass$_T$, Pt_T);

V05→Fill(V0Adecision$_T$, $V0Cdecision_T$);

V0AADA5→Fill(V0Adecision$_T$, $ADAdecision_T$);

V0CADC5→Fill(V0Cdecision$_T$, $ADCdecision_T$);

hPIDtrk0trk5→Fill(PIDTPCPion$_T$[0], $PIDTPCPion_T$[1]);

PhiPhipi5→Fill(u1.Phi(),u2.Phi());

Thetapi5→Fill(u1.Theta(),u2.Theta());

Pt1Pt2pi5→Fill(u1.Pt(),u2.Pt());

if(VtxChi2$_T$ > 100)

masapi6→Fill(Mass$_T$);

MPtpi6→Fill(Mass$_T$, Pt_T);

V06→Fill(V0Adecision$_T$, $V0Cdecision_T$);

V0AADA6→Fill(V0Adecision$_T$, $ADAdecision_T$);

V0CADC6→Fill(V0Cdecision$_T$, $ADCdecision_T$);

hPIDtrk0trk6→Fill(PIDTPCPion$_T$[0], $PIDTPCPion_T$[1]);

PhiPhipi6→Fill(u1.Phi(),u2.Phi());

Thetapi6→Fill(u1.Theta(),u2.Theta());

Pt1Pt2pi6→Fill(u1.Pt(),u2.Pt());

//chi

//vtx

//ad

//v0

//pt

//likesign

//PID

//for

//gStyle→SetOptStat(0);

gStyle→SetOptTitle(0);

// gStyle→SetPalette(1);

//gStyle→SetCanvasColor(33);

//gStyle→SetFrameFillColor(18);

//piones

/* TCanvas *c27 = new TCanvas(”c27”,”masa”);

masapi0→SetLineColor(kBlack);

masapi0→Draw();

masapi1→SetLineColor(kBlue);

masapi1→Draw(”same”);

masapi2→SetLineColor(kRed);

masapi2→Draw(”same”);

```
masapi3→SetLineColor(kMagenta);
masapi3→Draw("same");
masapi4→SetLineColor(kPink);
masapi4→Draw("same");
masapi5→SetLineColor(kGreen);
masapi5→Draw("same");
masapi6→SetLineColor(kOrange);
masapi6→Draw("same");
*/
TCanvas *c31 = new TCanvas("c31","masa 1");
masapi0→Draw();
TCanvas *c32 = new TCanvas("c32","masa 1");
masapi1→Draw();
TCanvas *c33 = new TCanvas("c33","masa 1");
masapi2→Draw();
TCanvas *c34 = new TCanvas("c34","masa 1");
masapi3→Draw();
TCanvas *c35 = new TCanvas("c35","masa 1");
masapi4→raw();
TCanvas *c36 = new TCanvas("c36","masa 1");
masapi5→Draw();
TCanvas *c38 = new TCanvas("c38","masa 1");
masapi6→Draw();
TCanvas *c41 = new TCanvas("c41","masa 1");
MPtpi0→Draw("colz");
TCanvas *c42 = new TCanvas("c42","masa 1");
MPtpi1→Draw("colz");
TCanvas *c43 = new TCanvas("c43","masa 2");
MPtpi2→Draw("colz");
```

```
TCanvas *c44 = new TCanvas("c44","masa 3");
MPtpi3→Draw("colz");
TCanvas *c45 = new TCanvas("c45","masa 4");
MPtpi4→Draw("colz");
TCanvas *c46 = new TCanvas("c46","masa 5");
MPtpi5→Draw("colz");
TCanvas *c47 = new TCanvas("c47","masa 5");
MPtpi6→Draw("colz");
TCanvas *c51 = new TCanvas("c51","masa 1");
V00→Draw("colz");
TCanvas *c52 = new TCanvas("c52","masa 1");
V01→Draw("colz");
TCanvas *c53 = new TCanvas("c53","masa 2");
V02→Draw("colz");
TCanvas *c54 = new TCanvas("c54","masa 3");
V03→Draw("colz");
TCanvas *c55 = new TCanvas("c55","masa 4");
V04→Draw("colz");
TCanvas *c56 = new TCanvas("c56","masa 5");
V05→Draw("colz");
TCanvas *c57 = new TCanvas("c57","masa 5");
V06→Draw("colz");
TCanvas *c61 = new TCanvas("c61","masa 1");
V0AADA0→Draw("colz");
TCanvas *c62 = new TCanvas("c62","masa 1");
V0AADA1→Draw("colz");
TCanvas *c63 = new TCanvas("c63","masa 2");
V0AADA2→Draw("colz");
TCanvas *c64 = new TCanvas("c64","masa 3");
```

```
V0AADA3→Draw("colz");
TCanvas *c65 = new TCanvas("c65","masa 4");
V0AADA4→Draw("colz");
TCanvas *c26 = new TCanvas("c26","masa 5");
V0AADA5→Draw("colz");
TCanvas *c67 = new TCanvas("c67","masa 5");
V0AADA6→Draw("colz");
TCanvas *c71 = new TCanvas("c71","masa 1");
V0CADC0→Draw("colz");
TCanvas *c72 = new TCanvas("c72","masa 1");
V0CADC1→Draw("colz");
TCanvas *c73 = new TCanvas("c73","masa 2");
V0CADC2→Draw("colz");
TCanvas *c74 = new TCanvas("c74","masa 3");
V0CADC3→Draw("colz");
TCanvas *c75 = new TCanvas("c75","masa 4");
V0CADC4→Draw("colz");
TCanvas *c76 = new TCanvas("c76","masa 5");
V0CADC5→Draw("colz");
TCanvas *c77 = new TCanvas("c77","masa 5");
V0CADC6→Draw("colz");
TCanvas *c81 = new TCanvas("c81","masa 1");
hPIDtrk0trk0→Draw("colz");
TCanvas *c82 = new TCanvas("c82","masa 1");
hPIDtrk0trk1→Draw("colz");
TCanvas *c83 = new TCanvas("c83","masa 2");
hPIDtrk0trk2→Draw("colz");
TCanvas *c84 = new TCanvas("c84","masa 3");
hPIDtrk0trk3→Draw("colz");
```

```
TCanvas *c85 = new TCanvas("c85","masa 4");
hPIDtrk0trk4→Draw("colz");
TCanvas *c86 = new TCanvas("c86","masa 5");
hPIDtrk0trk5→Draw("colz");
TCanvas *c87 = new TCanvas("c87","masa 5");
hPIDtrk0trk6→Draw("colz");
TCanvas *c91 = new TCanvas("c91","masa 1");
PhiPhipi0→Draw("colz");
TCanvas *c92 = new TCanvas("c92","masa 1");
PhiPhipi1→Draw("colz");
TCanvas *c93 = new TCanvas("c93","masa 2");
PhiPhipi2→Draw("colz");
TCanvas *c94 = new TCanvas("c94","masa 3");
PhiPhipi3→Draw("colz");
TCanvas *c95 = new TCanvas("c95","masa 4");
PhiPhipi4→Draw("colz");
TCanvas *c96 = new TCanvas("c96","masa 5");
PhiPhipi5→Draw("colz");
TCanvas *c97 = new TCanvas("c97","masa 5");
PhiPhipi6→Draw("colz");
TCanvas *c11 = new TCanvas("c11","masa 1");
Thetapi0→Draw("colz");
TCanvas *c12 = new TCanvas("c12","masa 1");
Thetapi1→Draw("colz");
TCanvas *c13 = new TCanvas("c13","masa 2");
Thetapi2→Draw("colz");
TCanvas *c14 = new TCanvas("c14","masa 3");
Thetapi3→Draw("colz");
TCanvas *c15 = new TCanvas("c15","masa 4");
```

```
Thetapi4→Draw("colz");
TCanvas *c16 = new TCanvas("c16","masa 5");
Thetapi5→Draw("colz");
TCanvas *c17 = new TCanvas("c17","masa 5");
Thetapi6→Draw("colz");
TCanvas *c01 = new TCanvas("c01","masa 1");
Pt1Pt2pi0→Draw("colz");
TCanvas *c02 = new TCanvas("c02","masa 1");
Pt1Pt2pi1→Draw("colz");
TCanvas *c03 = new TCanvas("c03","masa 2");
Pt1Pt2pi→Draw("colz");
TCanvas *c04 = new TCanvas("c04","masa 3");
Pt1Pt2pi3→Draw("colz");
TCanvas *c05 = new TCanvas("c05","masa 4");
Pt1Pt2pi4→Draw("colz");
TCanvas *c06 = new TCanvas("c06","masa 5");
Pt1Pt2pi5→Draw("colz");
TCanvas *c07 = new TCanvas("c07","masa 5");
Pt1Pt2pi6→Draw("colz");
TFile OutputFile("18l-13.root","recreate");
OutputFile.cd();
masapi0 → Write();
masapi1→Write();
masapi2→Write();
masapi3→Write();
masapi4→Write();
masapi5→Write();
masapi6→Write();
MPtpi0→Write();
```

```
MPtpi1→Write();
MPtpi2→Write();
MPtpi3→Write();
MPtpi4→Write();
MPtpi5→Write();
MPtpi6→Write();
V00→Write();
V01→Write();
V02→Write();
V03→Write();
V04→Write();
V05→Write();
V06→Write();
V0AADA0→Write();
V0AADA1→Write();
V0AADA2→Write();
V0AADA3→Write();
V0AADA4→Write();
V0AADA5→Write();
V0AADA6→Write();
V0CADC0→Write();
V0CADC1→Write();
V0CADC2→Write();
V0CADC3→Write();
V0CADC4→Write();
V0CADC5→Write();
V0CADC6→Write();
hPIDtrk0trk0→Write();
hPIDtrk0trk1→Write();
```

```
hPIDtrk0trk2→Write();
hPIDtrk0trk3→Write();
hPIDtrk0trk4→Write();
hPIDtrk0trk5→Write();
hPIDtrk0trk6→Write();
PhiPhipi0→Write();
PhiPhipi1→Write();
PhiPhipi2→Write();
PhiPhipi3→Write();
PhiPhipi4→Write();
PhiPhipi5→Write();
PhiPhipi6→Write();
Thetapi0→Write();
Thetapi1→Write();
Thetapi2→Write();
Thetapi3→Write();
Thetapi4→Write();
Thetapi5→Write();
Thetapi6→Write();
Pt1Pt2pi0→Write();
Pt1Pt2pi1→Write();
Pt1Pt2pi2→Write();
Pt1Pt2pi3→Write();
Pt1Pt2pi4→Write();
Pt1Pt2pi5→Write();
Pt1Pt2pi6→Write();
OutputFile.Close();
```

A.2 Four pions

void analisis4mass()

TFile* f = new TFile("17k-ccup25-4pi.root");

$\mathrm{Int}_t RunNum_T = 0;$

$\mathrm{UShort}_t BunchCrossNumber_T = 0;$

$\mathrm{UInt}_t OrbitNumber_T = 0;$

$\mathrm{UInt}_t PeriodNumber_T = 0;$

$\mathrm{Bool}_t LikeSign_T;$

$\mathrm{Float}_t Mass_T = 0;$

$\mathrm{Float}_t Pt_T = 0;$

$\mathrm{Float}_t Rapidity_T = 0;$

$\mathrm{Float}_t Mass_T P = 0; //added$

$\mathrm{Float}_t Pt_T P = 0; //added$

$\mathrm{Float}_t Rapidity_T P = 0; //added$

$\mathrm{Float}_t Mass_T K = 0; //added$

$\mathrm{Float}_t Pt_T K = 0; //added$

$\mathrm{Float}_t Rapidity_T K = 0; //added$

$\mathrm{Int}_t V0Adecision_T = 0;$

$\mathrm{Int}_t V0Cdecision_T = 0;$

$\mathrm{Int}_t ADAdecision_T = 0;$

$\mathrm{Int}_t ADCdecision_T = 0;$

$\mathrm{Bool}_t UBAfired_T = 0;$

$\mathrm{Bool}_t UBCfired_T = 0;$

$\mathrm{Float}_t ZNAenergy_T = 0;$

$\mathrm{Float}_t ZNCenergy_T = 0;$

$\mathrm{Float}_t ZPAenergy_T = 0;$

$\mathrm{Float}_t ZPCenergy_T = 0;$

$\mathrm{Float}_t ZDCAtime_T[4];$

$\mathrm{Float}_t ZDCCtime_T[4];$

$\text{Float}_t PIDTPCPion_T[4];$

$//\text{Float}_t PIDTPCElectron_T[2];$

$\text{Float}_t PIDTPCKaon_T[4]; //added$

$\text{Float}_t PIDTPCProton_T[4]; //added$

$\text{Float}_t PIDTPCMuon_T[4]; //added$

$\text{Int}_t TPCsignal_T[4];$

$\text{Float}_t TrackP_T[4];$

$\text{Float}_t Vertex_T[3];$

$\text{Int}_t VtxContrib_T = 0;$

$\text{Float}_t VtxChi2_T, VtxNDF_T = 0;$

$\text{Float}_t SpdVertex_T[3];$

$\text{Int}_t SpdVtxContrib_T = 0;$

$\text{Int}_t Ntracklets_T = 0;$

$\text{Float}_t Phi_T = 0;$

$\text{Float}_t Phi_T P = 0; //added$

$\text{Float}_t Phi_T K = 0; //added$

$\text{Float}_t TrackEta_T[4];$

$\text{Float}_t TrackPhi_T[4];$

$\text{Float}_t TrackPx_T[4];$

$\text{Float}_t TrackPy_T[4];$

$\text{Float}_t TrackPz_T[4];$

$\text{Bool}_t ChipCut_T = 0;$

$\text{Int}_t ITSModuleInner_T[4];$

$\text{Int}_t ITSModuleOuter_T[4];$

$\text{RhoTree}\rightarrow\text{SetBranchAddress}(\text{"RunNum}_T\text{"}, RunNum_T);$

$\text{RhoTree}\rightarrow\text{SetBranchAddress}(\text{"PeriodNumber}_T\text{"}, PeriodNumber_T);$

$\text{RhoTree}\rightarrow\text{SetBranchAddress}(\text{"OrbitNumber}_T\text{"}, OrbitNumber_T);$

$\text{RhoTree}\rightarrow\text{SetBranchAddress}(\text{"BunchCrossNumber}_T\text{"}, BunchCrossNumber_T);$

$\text{RhoTree}\rightarrow\text{SetBranchAddress}(\text{"LikeSign}_T\text{"}, LikeSign_T);$

RhoTree→SetBranchAddress("Mass$_T$", $Mass_T$);

RhoTree→SetBranchAddress("Pt$_T$", Pt_T);

RhoTree→SetBranchAddress("Rapidity$_T$", $Rapidity_T$);

RhoTree→SetBranchAddress("Phi$_T$", Phi_T);

RhoTree→SetBranchAddress("Mass$_T P$", $Mass_T P$); //*added*

RhoTree→SetBranchAddress("Pt$_T P$", $Pt_T P$); //*added*

RhoTree→SetBranchAddress("Rapidity$_T P$", $Rapidity_T P$); //*added*

RhoTree→SetBranchAddress("Phi$_T P$", $Phi_T P$); //*added*

RhoTree→SetBranchAddress("Mass$_T K$", $Mass_T K$); //*added*

RhoTree→SetBranchAddress("Pt$_T K$", $Pt_T K$); //*added*

RhoTree→SetBranchAddress("Rapidity$_T K$", $Rapidity_T K$); //*added*

RhoTree→SetBranchAddress("Phi$_T K$", $Phi_T K$); //*added*

RhoTree→SetBranchAddress("ZNAenergy$_T$", $ZNAenergy_T$);

RhoTree→SetBranchAddress("ZNCenergy$_T$", $ZNCenergy_T$);

RhoTree→SetBranchAddress("ZPAenergy$_T$", $ZPAenergy_T$);

RhoTree→SetBranchAddress("ZPCenergy$_T$", $ZPCenergy_T$);

RhoTree→SetBranchAddress("ZDCAtime$_T$", $ZDCAtime_T$);

RhoTree→SetBranchAddress("ZDCCtime$_T$", $ZDCCtime_T$);

RhoTree→SetBranchAddress("PIDTPCPion$_T$", $PIDTPCPion_T$);

RhoTree→SetBranchAddress("PIDTPCProton$_T$", $PIDTPCProton_T$); //*added*

RhoTree→SetBranchAddress("PIDTPCKaon$_T$", $PIDTPCKaon_T$); //*added*

RhoTree→SetBranchAddress("TPCsignal$_T$", $TPCsignal_T$);

RhoTree→SetBranchAddress("TrackP$_T$", $TrackP_T$);

RhoTree→SetBranchAddress("TrackEta$_T$", $TrackEta_T$);

RhoTree→SetBranchAddress("TrackPhi$_T$", $TrackPhi_T$);

RhoTree→SetBranchAddress("TrackPx$_T$", $TrackPx_T$);

RhoTree→SetBranchAddress("TrackPy$_T$", $TrackPy_T$);

RhoTree→SetBranchAddress("TrackPz$_T$", $TrackPz_T$);

RhoTree→SetBranchAddress("VtxX$_T$", $Vertex_T[0]$);

RhoTree→SetBranchAddress("VtxY$_T$", $Vertex_T[1]$);

RhoTree→SetBranchAddress("VtxZ$_T$", $Vertex_T[2]$);

RhoTree→SetBranchAddress("VtxContrib$_T$", $VtxContrib_T$);

RhoTree→SetBranchAddress("VtxChi2$_T$", $VtxChi2_T$);

RhoTree→SetBranchAddress("VtxNDF$_T$", $VtxNDF_T$);

RhoTree→SetBranchAddress("SpdVtxX$_T$", $SpdVertex_T[0]$);

RhoTree→SetBranchAddress("SpdVtxY$_T$", $SpdVertex_T[1]$);

RhoTree→SetBranchAddress("SpdVtxZ$_T$", $SpdVertex_T[2]$);

RhoTree→SetBranchAddress("SpdVtxContrib$_T$", $SpdVtxContrib_T$);

RhoTree→SetBranchAddress("V0Adecision$_T$", $V0Adecision_T$);

RhoTree→SetBranchAddress("V0Cdecision$_T$", $V0Cdecision_T$);

RhoTree→SetBranchAddress("ADAdecision$_T$", $ADAdecision_T$);

RhoTree→SetBranchAddress("ADCdecision$_T$", $ADCdecision_T$);

RhoTree→SetBranchAddress("UBAfired$_T$", $UBAfired_T$);

RhoTree→SetBranchAddress("UBCfired$_T$", $UBCfired_T$);

RhoTree→SetBranchAddress("Ntracklets$_T$", $Ntracklets_T$);

RhoTree→SetBranchAddress("ChipCut$_T$", $ChipCut_T$);

TH1D *masapi0 = new TH1D("masapi0","Invariant mass pi+pi- and cuts; Mass(GeV/c2); Events",1000,0,20);

TH1D *masapi1 = new TH1D("masapi1","Invariant mass pi+pi- and cuts; Mass(GeV/c2); Events",1000,0,20);

TH1D *masapi2 = new TH1D("masapi2","Invariant mass pi+pi- and cuts; Mass(GeV/c2); Events",1000,0,20);

TH1D *masapi3 = new TH1D("masapi3","Invariant mass pi+pi- and cuts; Mass(GeV/c2); Events",1000,0,20);

TH1D *masapi4 = new TH1D("masapi4","Invariant mass pi+pi- and cuts; Mass(GeV/c2); Events",1000,0,20);

TH1D *masapi5 = new TH1D("masapi5","Invariant mass pi+pi- and cuts; Mass(GeV/c2); Events",1000,0,20);

```
TH1D *masapi6 = new TH1D("masapi6","Invariant mass pi+pi- and cuts; Mass(GeV/c2);
Events",1000,0,20);
/*TH2D *MPtpi1= new TH2D("MPtpi1", "Invariant Mass vs Pt; Mass (GeV/c2); Pt
(GeV/c)", 100, 0, 4, 100, 0, 3);
TH2D *MPtpi2= new TH2D("MPtpi2", "Invariant Mass vs Pt; Mass (GeV/c2); Pt
(GeV/c)", 100, 0, 4, 100, 0, 0.51);
TH2D *MPtpi3= new TH2D("MPtpi3", "Invariant Mass vs Pt; Mass (GeV/c2); Pt
(GeV/c)", 100, 0, 4, 100, 0, 0.51);
TH2D *MPtpi4= new TH2D("MPtpi4", "Invariant Mass vs Pt; Mass (GeV/c2); Pt
(GeV/c)", 100, 0, 4, 100, 0, 0.51);
TH2D *MPtpi5= new TH2D("MPtpi5", "Invariant Mass vs Pt; Mass (GeV/c2); Pt
(GeV/c)", 100, 0, 4, 100, 0, 0.51);
TH2D *MPtpi6= new TH2D("MPtpi6", "Invariant Mass vs Pt; Mass (GeV/c2); Pt
(GeV/c)", 100, 0, 4, 100, 0, 0.51);*/
/* TH2F *V01 = new TH2F("V01","V0A vs V0C; V0A;V0C",4,0,4,4,0,4);
TH2F *V02 = new TH2F("V02","V0A vs V0C; V0A;V0C",4,0,4,4,0,4);
TH2F *V03 = new TH2F("V03","V0A vs V0C; V0A;V0C",4,0,4,4,0,4);
TH2F *V04 = new TH2F("V04","V0A vs V0C; V0A;V0C",4,0,4,4,0,4);
TH2F *V05 = new TH2F("V05","V0A vs V0C; V0A;V0C",4,0,4,4,0,4);
TH2F *V06 = new TH2F("V06","V0A vs V0C; V0A;V0C",4,0,4,4,0,4); */
/* TH2F *V0AADA1 = new TH2F("V0AADA1","V0A vs ADA; V0A; ADA",4,0,4,4,0,4);
TH2F *V0AADA2 = new TH2F("V0AADA2","V0A vs ADA; V0A; ADA",4,0,4,4,0,4);
TH2F *V0AADA3 = new TH2F("V0AADA3","V0A vs ADA; V0A; ADA",4,0,4,4,0,4);
TH2F *V0AADA4 = new TH2F("V0AADA4","V0A vs ADA; V0A; ADA",4,0,4,4,0,4);
TH2F *V0AADA5 = new TH2F("V0AADA5","V0A vs ADA; V0A; ADA",4,0,4,4,0,4);
TH2F *V0AADA6 = new TH2F("V0AADA6","V0A vs ADA; V0A; ADA",4,0,4,4,0,4);
*/
/* TH2F *V0CADC1= new TH2F("V0CADC1","V0C vs ADC; V0C; ADC",4,0,4,4,0,4);
TH2F *V0CADC2= new TH2F("V0CADC2","V0C vs ADC; V0C; ADC",4,0,4,4,0,4);
```

```
TH2F *V0CADC3= new TH2F("V0CADC3","V0C vs ADC; V0C; ADC",4,0,4,4,0,4);
TH2F *V0CADC4= new TH2F("V0CADC4","V0C vs ADC; V0C; ADC",4,0,4,4,0,4);
TH2F *V0CADC5= new TH2F("V0CADC5","V0C vs ADC; V0C; ADC",4,0,4,4,0,4);
TH2F *V0CADC6= new TH2F("V0CADC6","V0C vs ADC; V0C; ADC",4,0,4,4,0,4);
*/
/* TH2F *hPIDtrk0trk1 = new TH2F("hPIDtrk0trk1","PIDtrack0 vs PIDtrack1; PID-
track0; PIDtrack1",100,-4,4,100,-4,4);
TH2F *hPIDtrk0trk2 = new TH2F("hPIDtrk0trk2","PIDtrack0 vs PIDtrack1; PID-
track0; PIDtrack1",100,-4,4,100,-4,4);
TH2F *hPIDtrk0trk3 = new TH2F("hPIDtrk0trk3","PIDtrack0 vs PIDtrack1; PID-
track0; PIDtrack1",100,-4,4,100,-4,4);
TH2F *hPIDtrk0trk4 = new TH2F("hPIDtrk0trk4","PIDtrack0 vs PIDtrack1; PID-
track0; PIDtrack1",100,-4,4,100,-4,4);
TH2F *hPIDtrk0trk5 = new TH2F("hPIDtrk0trk5","PIDtrack0 vs PIDtrack1; PID-
track0; PIDtrack1",100,-4,4,100,-4,4);
TH2F *hPIDtrk0trk6 = new TH2F("hPIDtrk0trk6","PIDtrack0 vs PIDtrack1; PID-
track0; PIDtrack1",100,-4,4,100,-4,4);
*/
for (Int_t ev = 0; ev < RhoTree→GetEntries();ev++)
RhoTree→GetEntry(ev);
//piones
if(LikeSign_T == 0)
masapi0→Fill(Mass_T);
//MPtpi1→Fill(Mass_T, Pt_T);
//V01→Fill(V0Adecision_T, V0Cdecision_T);
//V0AADA1→Fill(V0Adecision_T, ADAdecision_T);
//V0CADC1→Fill(V0Cdecision_T, ADCdecision_T);
//hPIDtrk0trk1→Fill(PIDTPCPion_T[0], PIDTPCPion_T[1]);
if(PIDTPCPion_T[0] ** 2 + PIDTPCPion_T[1] ** 2 < 4)
```

masapi1→Fill(Mass$_T$);

if(Pt$_T$ < 1)

masapi2→Fill(Mass$_T$);

//MPtpi2→Fill(Mass$_T$, Pt_T);

//V02→Fill(V0Adecision$_T$, $V0Cdecision_T$);

//V0AADA2→Fill(V0Adecision$_T$, $ADAdecision_T$);

//V0CADC2→Fill(V0Cdecision$_T$, $ADCdecision_T$);

//hPIDtrk0trk2→Fill(PIDTPCPion$_T$[0], $PIDTPCPion_T$[1]);

if(V0Adecision$_T$ == $0V0Cdecision_T$ == 0)

masapi3→Fill(Mass$_T$);

//MPtpi3→Fill(Mass$_T$, Pt_T);

//V03→Fill(V0Adecision$_T$, $V0Cdecision_T$);

//V0AADA3→Fill(V0Adecision$_T$, $ADAdecision_T$);

//V0CADC3→Fill(V0Cdecision$_T$, $ADCdecision_T$);

//hPIDtrk0trk3→Fill(PIDTPCPion$_T$[0], $PIDTPCPion_T$[1]);

if(ADAdecision$_T$ == $0ADCdecision_T$ == 0)

masapi4→Fill(Mass$_T$);

//MPtpi4→Fill(Mass$_T$, Pt_T);

//V04→Fill(V0Adecision$_T$, $V0Cdecision_T$);

//V0AADA4→Fill(V0Adecision$_T$, $ADAdecision_T$);

//V0CADC4→Fill(V0Cdecision$_T$, $ADCdecision_T$);

//hPIDtrk0trk4→Fill(PIDTPCPion$_T$[0], $PIDTPCPion_T$[1]);

if(Vertex$_T$[2] < $10Vertex_T$[2] > −10)

masapi5→Fill(Mass$_T$);

// MPtpi5→Fill(Mass$_T$, Pt_T);

//V05→Fill(V0Adecision$_T$, $V0Cdecision_T$);

//V0AADA5→Fill(V0Adecision$_T$, $ADAdecision_T$);

//V0CADC5→Fill(V0Cdecision$_T$, $ADCdecision_T$);

//hPIDtrk0trk5→Fill(PIDTPCPion$_T$[0], $PIDTPCPion_T$[1]);

```
if(VtxChi2_T > 100)
masapi6→Fill(Mass_T);
//MPtpi6→Fill(Mass_T, Pt_T);
//V06→Fill(V0Adecision_T, V0Cdecision_T);
//V0AADA6→Fill(V0Adecision_T, ADAdecision_T);
//V0CADC6→Fill(V0Cdecision_T, ADCdecision_T);
//hPIDtrk0trk6→Fill(PIDTPCPion_T[0], PIDTPCPion_T[1]);
//chi
//vtx
//ad
//v0
//pt
//likesign
//PID
//for
//gStyle→SetOptStat(0);
//gStyle→SetOptTitle(0);
// gStyle→SetPalette(1);
//gStyle→SetCanvasColor(33);
//gStyle→SetFrameFillColor(18);
//piones
/*
TCanvas *c27 = new TCanvas("c27","masa");
masapi0→SetLineColor(kBlack);
masapi0→Draw();
masapi1→SetLineColor(kBlue);
masapi1→Draw("same");
masapi2→SetLineColor(kRed);
masapi2→Draw("same");
```

```
masapi3→SetLineColor(kMagenta);
masapi3→Draw(”same”);
masapi4→SetLineColor(kPink);
masapi4→Draw(”same”);
masapi5→SetLineColor(kGreen);
masapi5→Draw(”same”);
masapi6→SetLineColor(kOrange);
masapi6→Draw(”same”);
*/
TCanvas *c21 = new TCanvas(”c21”,”masa 1”);
masapi0→Draw();
TCanvas *c22 = new TCanvas(”c22”,”masa 1”);
masapi6→SetLineColor(kBlack);
masapi1→Draw();
TCanvas *c23 = new TCanvas(”c23”,”masa 1”);
masapi2→SetLineColor(kBlue);
masapi2→Draw();
TCanvas *c24 = new TCanvas(”c24”,”masa 1”);
masapi3→SetLineColor(kRed);
masapi3→Draw();
TCanvas *c25 = new TCanvas(”c25”,”masa 1”);
masapi4→SetLineColor(kGreen);
masapi4→Draw();
TCanvas *c26 = new TCanvas(”c26”,”masa 1”);
masapi5→SetLineColor(kPink);
masapi5→Draw();
TCanvas *c28 = new TCanvas(”c28”,”masa 1”);
masapi6→SetLineColor(kOrange);
masapi6→Draw();
```

```
/* TCanvas *c22 = new TCanvas("c22","masa 1");
MPtpi1→Draw("colz");
TCanvas *c23 = new TCanvas("c23","masa 2");
MPtpi2→Draw("colz");
TCanvas *c24 = new TCanvas("c24","masa 3");
MPtpi3→Draw("colz");
TCanvas *c25 = new TCanvas("c25","masa 4");
MPtpi4→Draw("colz");
TCanvas *c26 = new TCanvas("c26","masa 5");
MPtpi5→Draw("colz");
TCanvas *c27 = new TCanvas("c27","masa 5");
MPtpi6→Draw("colz"); */
/* TCanvas *c22 = new TCanvas("c22","masa 1");
V01→Draw("colz");
TCanvas *c23 = new TCanvas("c23","masa 2");
V02→Draw("colz");
TCanvas *c24 = new TCanvas("c24","masa 3");
V03→Draw("colz");
TCanvas *c25 = new TCanvas("c25","masa 4");
V04→Draw("colz");
TCanvas *c26 = new TCanvas("c26","masa 5");
V05→Draw("colz");
TCanvas *c27 = new TCanvas("c27","masa 5");
V06→Draw("colz"); */ /* TCanvas *c22 = new TCanvas("c22","masa 1");
V0AADA1→Draw("colz");
TCanvas *c23 = new TCanvas("c23","masa 2");
V0AADA2→Draw("colz");
TCanvas *c24 = new TCanvas("c24","masa 3");
V0AADA3→Draw("colz");
```

```
TCanvas *c25 = new TCanvas("c25","masa 4");
V0AADA4→Draw("colz");
TCanvas *c26 = new TCanvas("c26","masa 5");
V0AADA5→Draw("colz");
TCanvas *c27 = new TCanvas("c27","masa 5");
V0AADA6→Draw("colz"); */ /* TCanvas *c22 = new TCanvas("c22","masa 1");
V0CADC1→Draw("colz");
TCanvas *c23 = new TCanvas("c23","masa 2");
V0CADC2→Draw("colz");
TCanvas *c24 = new TCanvas("c24","masa 3");
V0CADC3→Draw("colz");
TCanvas *c25 = new TCanvas("c25","masa 4");
V0CADC4→Draw("colz");
TCanvas *c26 = new TCanvas("c26","masa 5");
V0CADC5→Draw("colz");
TCanvas *c27 = new TCanvas("c27","masa 5");
V0CADC6→Draw("colz"); */
/* TCanvas *c22 = new TCanvas("c22","masa 1");
hPIDtrk0trk1→Draw("colz");
TCanvas *c23 = new TCanvas("c23","masa 2");
hPIDtrk0trk2→Draw("colz");
TCanvas *c24 = new TCanvas("c24","masa 3");
hPIDtrk0trk3→Draw("colz");
TCanvas *c25 = new TCanvas("c25","masa 4");
hPIDtrk0trk4→Draw("colz");
TCanvas *c26 = new TCanvas("c26","masa 5");
hPIDtrk0trk5→Draw("colz");
TCanvas *c27 = new TCanvas("c27","masa 5");
hPIDtrk0trk6→Draw("colz"); */
```

```
TFile OutputFile("17k-25.root","recreate");
OutputFile.cd();
masapi0→Write();
masapi1→Write();
masapi2→Write();
masapi3→Write();
masapi4→Write();
masapi5→Write();
masapi6 → Write();
OutputFile.Close();
```